UNIVERSITY OF OKLAHOMA

GRADUATE COLLEGE

EXPERIMENTAL STUDY OF GAS INJECTION ENHANCED OIL RECOVERY IN SHALE RESERVOIRS

A THESIS

SUBMITTED TO THE GRADUATE FACULTY

in partial fulfillment of the requirements for the

Degree of

MASTER OF SCIENCE

By

BYEUNGJU MIN
Norman, Oklahoma
2019

EXPERIMENTAL STUDY OF GAS INJECTION ENHANCED OIL RECOVERY IN SHALE RESERVOIRS

A THESIS APPROVED FOR THE
MEWBOURNE SCHOOL OF PETROLEUM AND GEOLOGICAL ENGINEERING

BY THE COMMITTEE CONSISTING OF

Dr. Carl Sondergeld, Chair

Dr. Chandra Rai

Dr. Mark Curtis

Dedicated to

My advisors, friends, and family

Table of contents

List of tables

List of figures

Abstract

Miscible gas injection enhanced oil recovery (huff-n-puff gas injection) has received increased attention especially in the unconventional plays like the Eagle Ford, where oil recovery is as low as 5 – 10% (Sheng, 2015). An increase in 1% of recovery in the Eagle Ford could realize a potential of 2.3 billion barrels of oil, which has an enormous economic value. Laboratory investigation of huff-n-puff gas injection can help in the systematic evaluation of different factors affecting the recovery performance of huff-n-puff gas injection operations. The focus of this study is to evaluate the efficacy of huff-n-puff gas injection in the Eagle Ford..

Eagle Ford shale samples were placed inside the a high-pressure vessel and different types of gas: carbon dioxide (CO_2,) methane (C1), ethane (C2), C1:C2 (72:28) mixture, C1:C2 (95:5) mixture, and field gas were injected at various pressures (1000 psi below MMP, MMP, and 1000 psi above MMP) with various soaking time of (1 hr, 3 hr and 6 hr). Nuclear magnetic resonance (NMR), HAWK source rock analysis, and gas chromatography (GC), were performed to quantify measurable changes in produced and residual hydrocarbons in preserved Eagle Ford shale samples.

Various controlling factors such as minimum miscibility pressure (MMP), surface area, soaking time, injection pressure, injection gas rate, and type of injection gas on huff-n-puff gas injection performance were evaluated.

Vanishing Interfacial Tension technique (VIT) was used to measure MMP for the Eagle Ford oil. MMP values with different types of gas: carbon dioxide (CO_2,) methane (C1), ethane (C2), C1:C2 (72:28) mixture, and field gas were measured to be 2500 psi, 6000 psi, 1000 psi, 3500 psi, and

3000 psi, respectively. Methane concentration plays a major role in MMP. As methane concentration increased, MMP also increased.

Surface area studies showed that after 5 huff-n-puff cycles, the recovery from samples with 7-8 mm and 0.9-2 mm sample sizes were 61% and 42%, respectively. Smaller sample size yields a higher recovery due to more surface area and better access to the small pores, which indicates the importance of stimulated reservoir volume (SRV).

When soaking time is compared per cycle, 6 hr soaking time yields the highest recovery compared to 1 hr or 3 hr soaking time. Longer soaking time also produced slightly heavier hydrocarbons. However, when residence time (soaking time + production time) is considered, there is no significant difference in ultimate recovery. This result suggested that longer soaking time seems to be a better economical choice due to the need for fewer injection cycles.

Injection pressure above MMP yields a higher recovery compared to pressure below MMP. Injection pressure also determines the fraction of hydrocarbons mobilized. When injection pressure was 1000 psi above MMP, mobilized hydrocarbon included up to C25. However, when injection pressure was 1000 psi below MMP, mobilized hydrocarbon was limited to C19 and below. Excessive pressure above MMP did not yield additional recovery in 7-8mm size samples. In addition, the effect of injection rate was investigated. High injection gas rate lead to better recovery (36%) than low injection rate (23%).

Our study indicates that gas composition has strong effect on the recovery factor. At cycle 3, with 7-8 mm sized particles, P=1000 psi above MMP and T=150°F, one hour soaking, and one hour production time, ethane showed the best performance of all the gases (40% recovery). CO_2 performed the second best (32%). C1:C2(72:28) mixture and field gas exhibit the similar recovery (24% and 21%, respectively). C1:C2(95:5) mixture showed the worst recovery (11%). This highlights the potential benefits of enriching injection gas.

Chapter 1: Introduction

1.1 Motivation and problem statement

According to 2018 ExxonMobil's energy outlook, energy demand will grow 25% by 2040 due to the population growth, income growth, and expansion of global middle class (India, China and Asia Pacific). This growth in overall demand in energy and the depletion of US conventional fields drive interests in unconventional resources such as tight reservoirs and organic shales . With the help of new technologies such as multi-stage hydraulic fracturing and horizontal drilling, U.S. oil production has grown from 5.6 million barrels per day(bbl/d) in 2006 to 11.9 million bbl/d in 2019 **(Fig. 1)**.

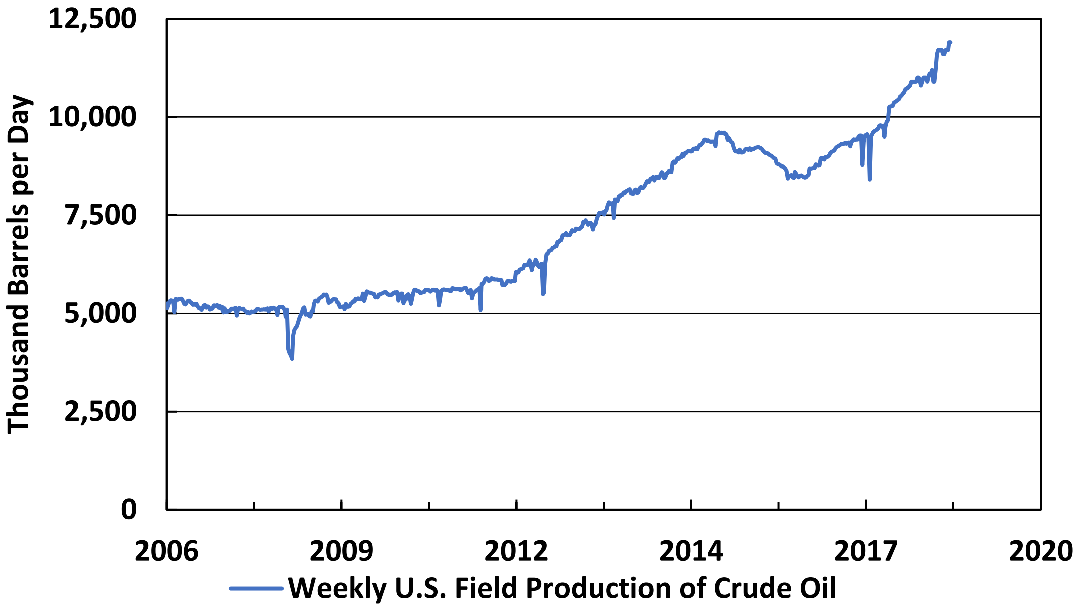

Figure 1: U.S. crude oil production history since 2006 (EIA 2019). Note that U.S. oil production has grown from 5.6MMbbl/d in 2006 to 11.9MMbbl/d in 2019

The main problem in producing from tight reservoirs and organic shales is sustainability (Ma, 2015). These unconventional wells initially exhibit high production rates but show rapid production decline rates over the first few years. This results in recovery factors of liquid rich unconventional plays to be quite low, i.e. 5-10% (Sheng, 2015; Hoffman and Evans 2016). Thus, exploration and development of new wells are necessary to maintain production. However, when it comes to compare the incremental cost, more permanent and economical solution to the problem would be to maximize the recovery of existing wells. There are numerous ways to increase the recovery factor including refracturing, waterflooding, thermal injection, surfactant injection, gas injection, etc. In this project, my focus is to evaluate the gas injection performance in liquid rich shale reservoirs.

Research interests in miscible gas injection in liquid rich shale was sparked by EOG Resources disclosing that it had a found a way to get from 30 to 70% more oil from Eagle Ford shale wells by injecting natural gas (**Fig. 2**).

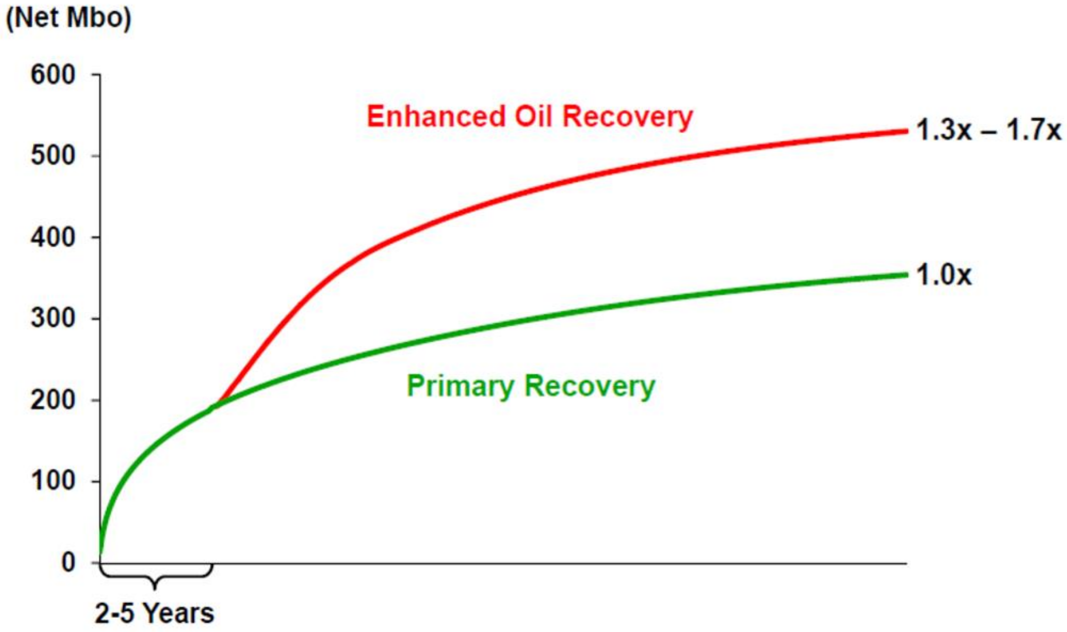

Figure 2: Reported expected recovery from huff-n-puff gas injection into the Eagle Ford (Thomas et al. 2016). Note the EOR increased oil recovery by 30 to 70%.

Numerous experimental and numerical research efforts have focused on the performance of gas injection huff-n-puff EOR in liquid rich shale. However, most of previous research on the performance of gas injection was focused on CO_2 injection or single component gas; primarily huff-n-puff tests on re-saturated samples **(**Hawthorne et al, 2013; Yu, 2016). Limited experimental studies were conducted using actual field gas or mixed gas such as C1: C2(72:28) or preserved cores.

1.2 Scope of the thesis

The focus of this thesis is to evaluate the efficacy of huff-n-puff gas injection in a liquid rich shale using preserved core samples. Various controlling factors such as minimum miscibility pressure (MMP), surface area, soaking time, production time, injection pressure, injection gas rate (pressure profile) and types of injection gas used in huff-n-puff gas injection performance were evaluated. Comparison is made by observing the difference in the recovery of HCs in preserved rock core samples. This study helps to understand the physics of miscible gas injection EOR and improve the screening criteria of huff-n-puff operations as well.

1.3 Organization of the thesis

This thesis is divided into five chapters and is presented as follows:

- Chapter 1; introduces the motivation, problem statement and describe the scope of this study.
- Chapter 2; includes literature reviews on gas injection EOR and the field study in unconventional reservoirs.
- Chapter 3; describes the details of the equipment, methodologies, and experimental procedures for MMP and huff-n-puff tests.
- Chapter 4; discusses the result and analyses of the study.
- Chapter 5; presents the conclusion and the most significant findings.

Chapter 2: Background Research and Literature Review

2.1 Cyclic gas injection (huff-n-puff gas injection)

Cyclic gas injection, commonly known as huff-n-puff gas injection, can be applied as the secondary recovery process or as tertiary recovery process after water flooding. Huff-n-puff gas injection is primarily operated for recovery of medium and light oil (17-38^{o}API) (Yu, 2016). Huff-n-puff gas injection is a single well operation involves three phases as shown in **Fig. 3:**

1. The injection phase (huff) – gas is injected into reservoir
2. The soak phase (huff) – the well is shut in to allow injected gas to dissipate and dissolve into the reservoir oil
3. Production phase (puff) – the oil and injected gas are produced

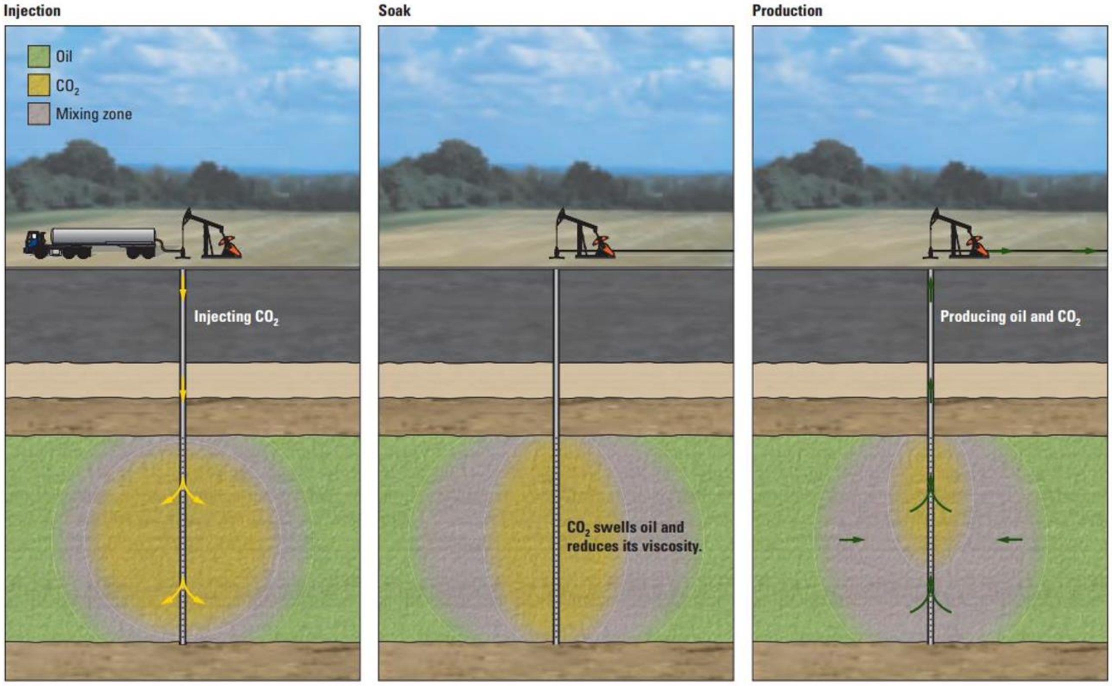

Figure 3: Huff-n-puff gas (CO_2) injection is a single well operation involving three phases: injection, soak and production (Al-mjeni et al. 2010).

2.2 Recovery mechanism of huff-n-puff gas injection

Various recovery mechanisms of huff-n-puff gas injection are summarized: (Holm and Josendal 1974; Stalkup 1987; Lansangan and Smith 1993; Ghedan 2009; Tabrizy and Hamouda 2014; Yin 2015 and Alharthy et al. 2018.)

- As injected gas dissolves into oil, viscosity reduces
- Solution gas also causes the swelling of oil volume
- Gas vaporizes and extracts hydrocarbons from oil
- Gas pressurizes the reservoir and gives more energy to drive fluids to the well
- Interfacial tension reduction due to miscibility
- Altering matrix/fracture interface wettability
- Favorably changing of oil and water phase density to reduce gravity segregation

However, the recovery mechanisms of huff-n-puff gas injection in liquid rich shale reservoir cannot be considered the same as those in conventional reservoirs. Since petrophysical properties, reservoir fluid thermodynamics and mass transport mechanisms are different in unconventional reservoirs (Wang et al. 2017). Alharthy et al. (2018) illustrated sequence of mass-transports events during huff-n-puff EOR process to extract hydrocarbons from the tight matrix (**Fig. 4**).

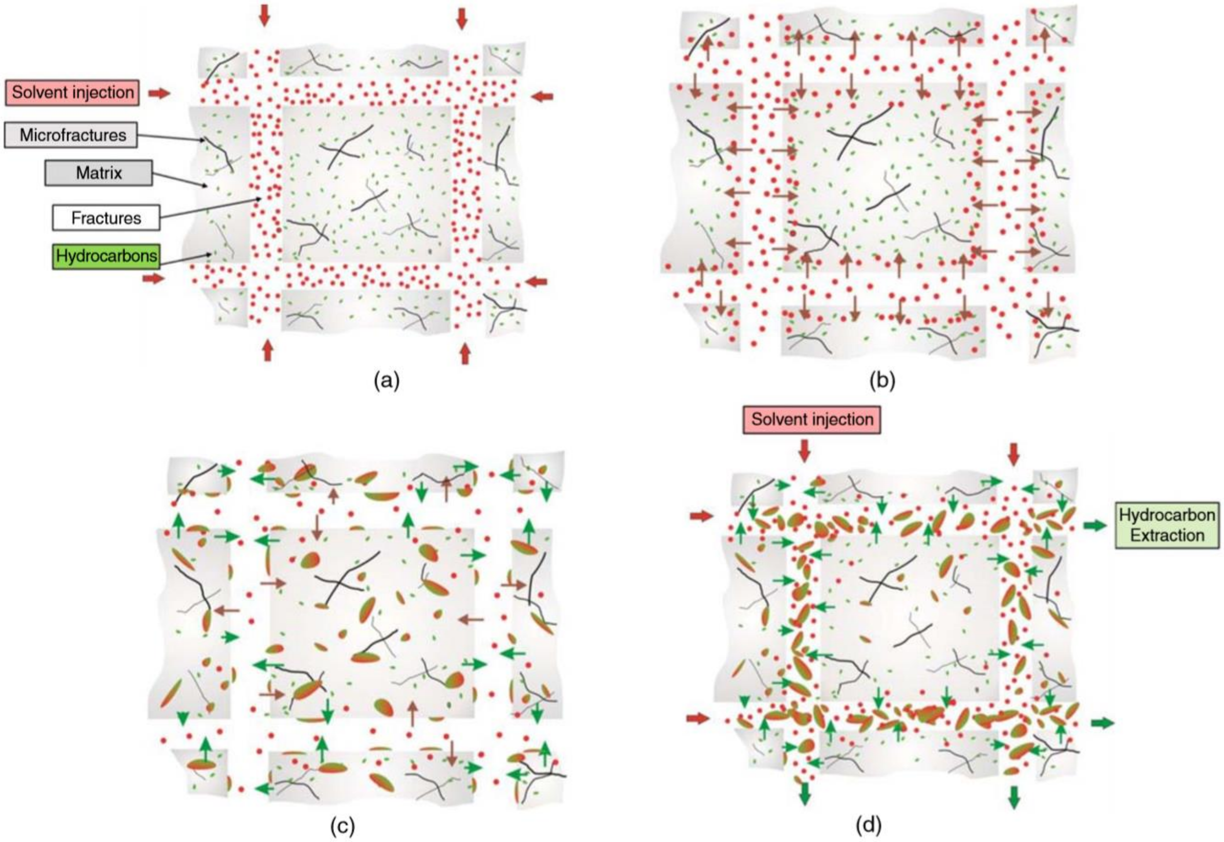

Figure 4: Sequence of mass transport events during huff-n-puff in tight rocks. (a) Represents the "huff" phase when solvent gas is injected into the well and transported through fracture network. During this stage, pressure gradient controls the transport of solvent into the matrix/fracture interface. (b) Represents the early soaking phase when solvent gas penetrates limited rock matrix and re-pressurizes. During this stage, pressure gradient still dominates. (c) Represents late soaking stage when the solvent penetrates further into the rock matrix through diffusive/advective mass transfer with molecular diffusion as the dominant flux. During this stage, oil swelling, viscosity reduction, and IFT reduction occur. As oil swells, the pressure increases slightly causing a local pressure gradient. This could accelerate oil extraction from the matrix through microfractures. (d) Represents "puff" phase when injected solvent gas mix with extracted oil which has been extracted due to oil swelling from microfractures. Gas/Oil mixture is mobilized to wellbore through main fracture network (Alharthy et al. 2018).

2.3 Literature review of huff-n-puff gas injection in unconventional reservoirs

Kovscek et al. (2008) conducted a CO_2 injection experiments with siliceous shale (0.02-1.3 mD permeability range and 30-40% porosity range) to compare recovery at near miscible condition and immiscible condition. X-ray CT scanning was utilized to monitor the recovery. The summary of the result is shown in **Table 1**. Authors suggested that immiscible CO_2 injection maybe technically feasible EOR method in shale, since the recovery from near miscible condition was not substantially different from immiscible conditions. However, it is worth noting that recovery from countercurrent flow (recovery from volumetric expansion of the oil phase) is greater than recovery from cocurrent flow (recovery from convective dispersion mechanism) under miscible condition.

Table 1: Summary of tests 1, 2 and 3. Note that total oil recovery from immiscible conditions (test 1 and test 2) are slightly less than total oil recovery from miscible conditions (test 3) (Kovscek et al. 2008).

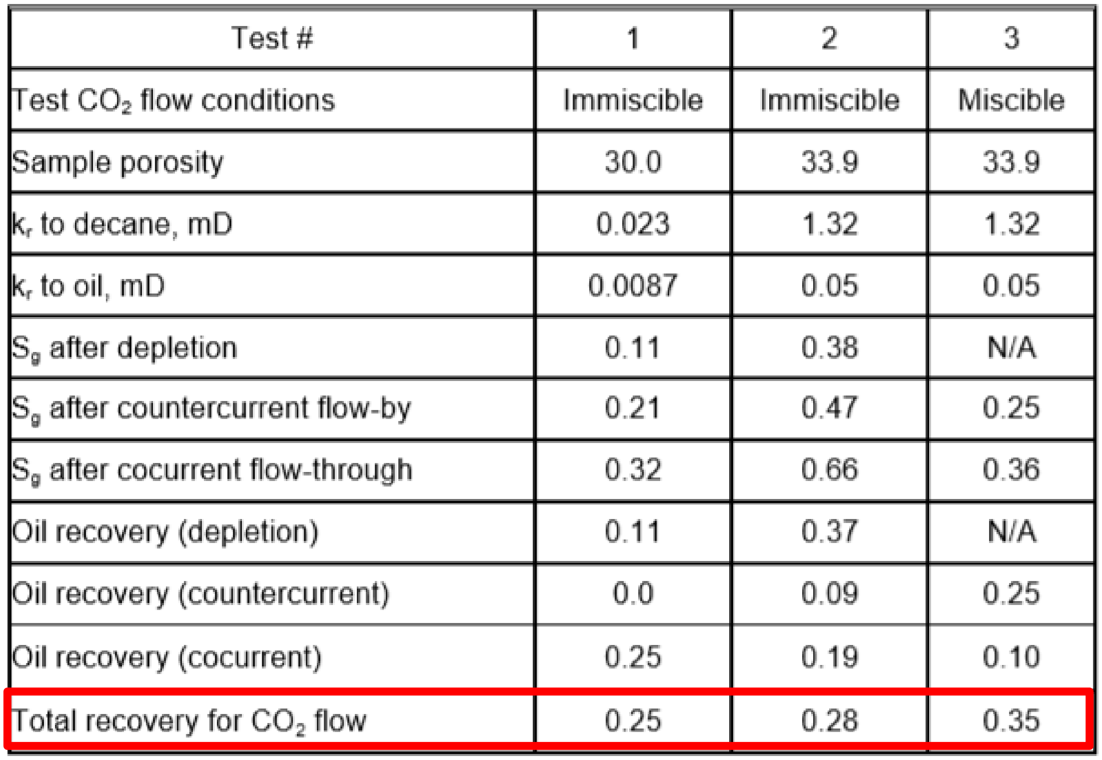

Test #	1	2	3
Test CO_2 flow conditions	Immiscible	Immiscible	Miscible
Sample porosity	30.0	33.9	33.9
k_r to decane, mD	0.023	1.32	1.32
k_r to oil, mD	0.0087	0.05	0.05
S_g after depletion	0.11	0.38	N/A
S_g after countercurrent flow-by	0.21	0.47	0.25
S_g after cocurrent flow-through	0.32	0.66	0.36
Oil recovery (depletion)	0.11	0.37	N/A
Oil recovery (countercurrent)	0.0	0.09	0.25
Oil recovery (cocurrent)	0.25	0.19	0.10
Total recovery for CO_2 flow	0.25	0.28	0.35

Song and Yang (2013) experimentally and numerically evaluated the performance of CO_2 huff-n-puff process. As received samples from Bakken formation (permeability range of 0.27-0.83 mD and 19-23% porosity range) were saturated with reservoir oil. Four different recovery schemes (waterflooding, CO_2 huff-n-puff in immiscible, near miscible, and miscible conditions) were evaluated experimentally. The waterflooding yielded higher recovery than immiscible CO_2 huff-n-puff, while both near miscible and miscible condition had better recovery than waterflooding. Numerical simulation was tuned with experimental results and sensitivity analysis of injection pressure and soaking time was performed. Simulation suggested that higher injection pressure improved oil recovery in only the first four cycles. Longer soaking time increased recovery up to 6 hours of soaking time, further increasing soaking time did not yield additional recovery (**Fig. 5**).

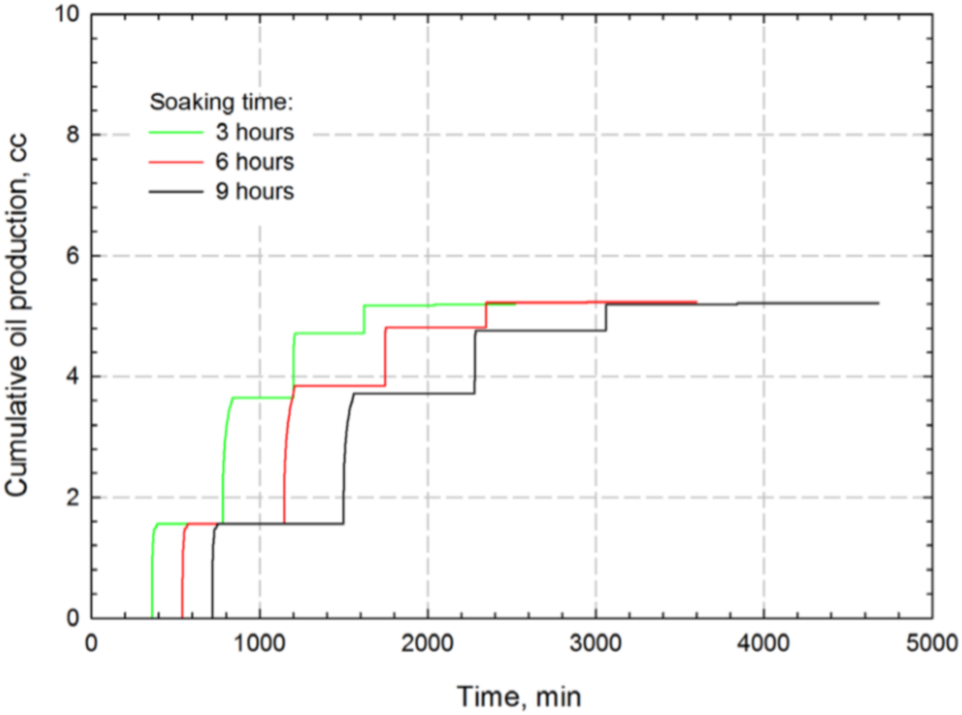

Figure 5: Simulated production profiles with different soaking times of miscible CO_2 huff-n-puff process (Song and Yang 2013). Note that further increasing soaking time did not yield additional recovery.

Gamadi et al. (2013) investigated effects of injection pressure in N_2 huff-n-puff experiments. Samples were Barnett, Marcos and Eagle Ford shales 1.5” in diameter and 2” in length. Mineral oil (Soltrol 130) was used to saturate at 2000 psi for 48 hours. The results suggest that recovery was high when the injection pressure was high due to large pressure drawdown during the production phase. They also found that Eagle Ford shale had the highest recovery of all samples, suggesting the better potential of gas EOR in Eagle Ford shale (**Fig. 6**). This may due to the Eagle Ford having favorable pore sizes and transport properties. The effect of soaking time was also investigated. A longer soaking time lead to a higher recovery.

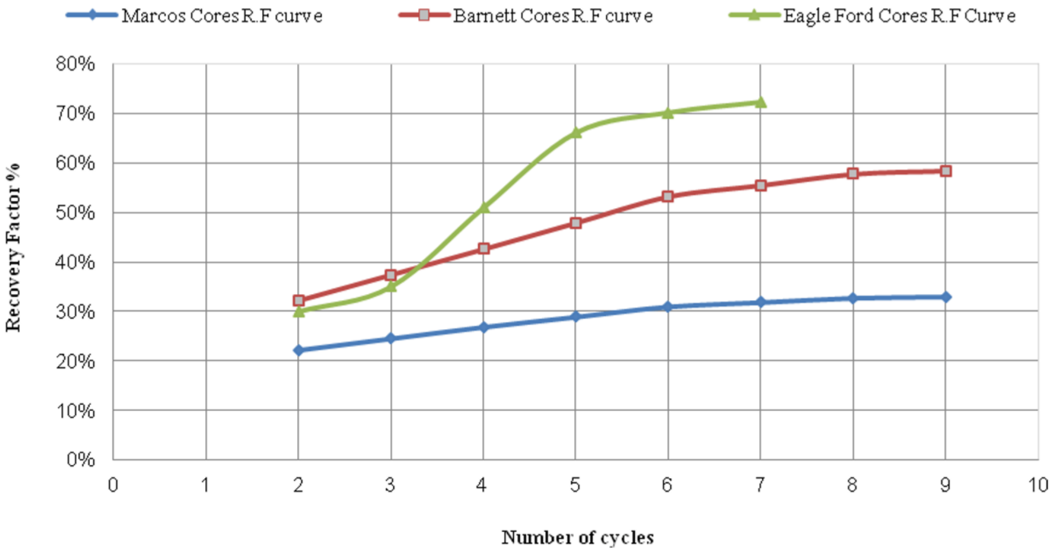

Figure 6: Performance of nitrogen huff-n-puff at near miscible condition as function of number of cycles for various shale formations (Gamadi et al. 2013). Note that Eagle Ford cores performed the best compared to Barnett cores and Marcos cores, suggesting the better potential for huff-n-puff in the Eagle Ford.

Hawthorne et al. (2013) conducted a series of CO_2 huff-n-puff experiments on middle Bakken samples (0.002-0.04 md permeability and 4.5-8.1% porosity) and on lower and upper Bakken formation samples saturated with Bakken crude oil. The results suggest that middle Bakken sample shows the best recovery of three Bakken formations. Unexpectedly, despite being very tight source rocks, lower and upper Bakken sample achieved high recovery with longer exposure time and high surface area to volume ratio (**Fig. 7**).

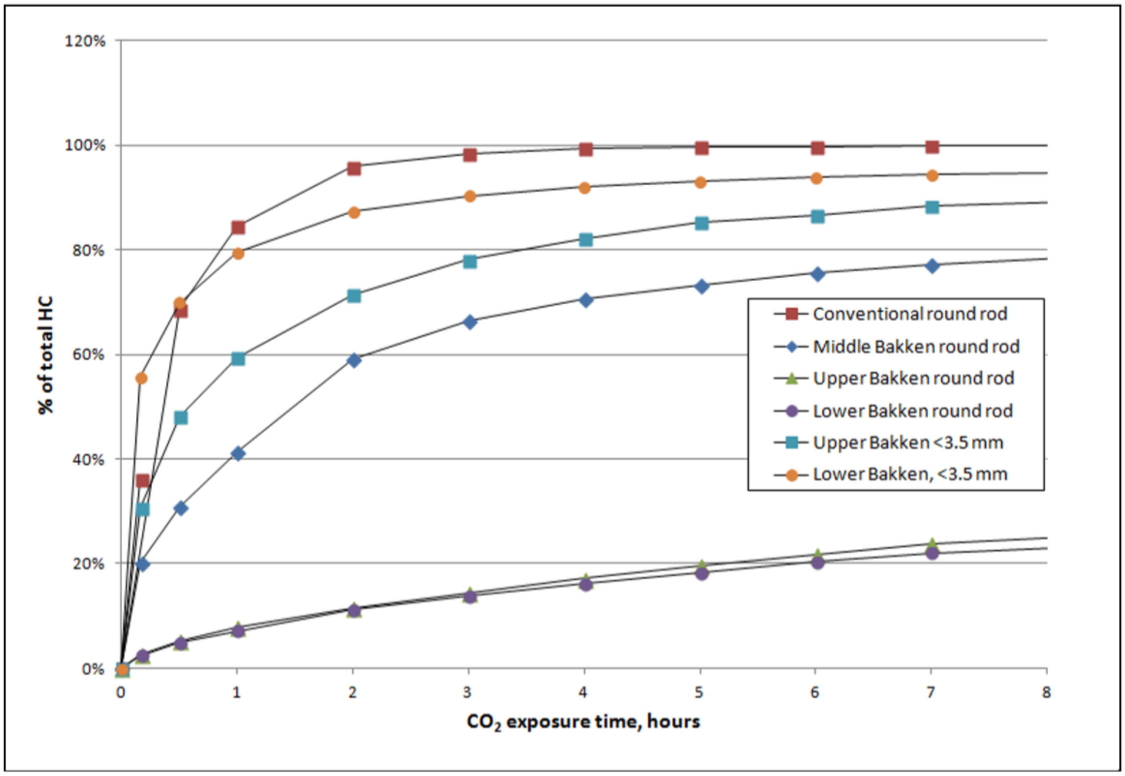

Figure 7: CO_2 mobilization of hydrocarbons from Upper Bakken, Middle Bakken, Lower Bakken (all from the same borehole), and a conventional reservoir rock at 5000 psi and 110°C. "Rounds rods" represents a cylinder with a diameter of 10mm X 40mm long. "< 3.5mm" indicates rock crushed to pass a 3.5mm screen (Hawthorne et al. 2013).

Sorensen et al. (2014) developed detailed petrophysical and geological models for the Middle and Lower Bakken formation based on field characterization, well log interpretation, and laboratory core analysis (SEM, ultraviolet fluorescence, and optical microscopy). These models and simulations were used to examine the potential effectiveness of CO_2 based EOR. The results indicate that production can be increased by 43% to 58% compared to case without CO_2 injection as shown in **Fig. 8**.

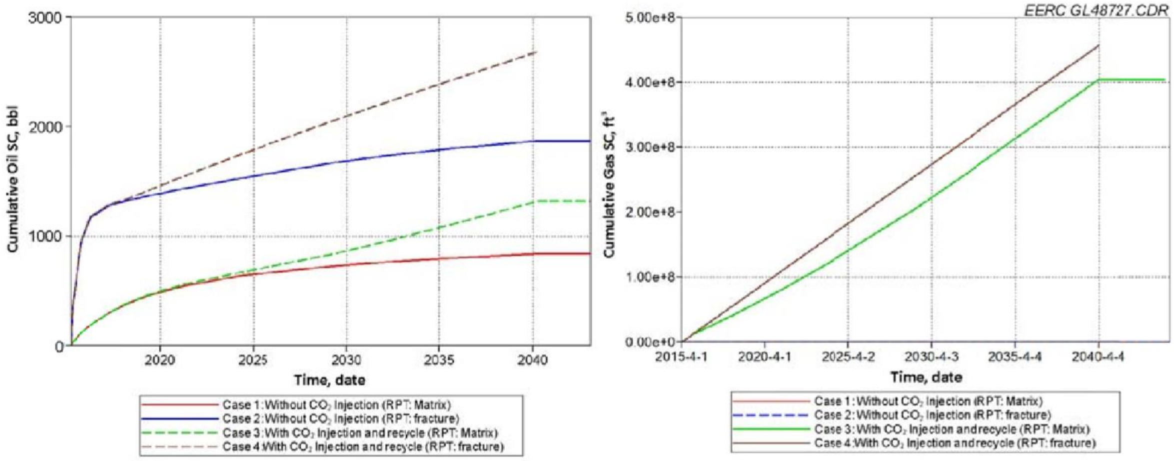

Figure 8: Simulation results for four cases. Left: Cumulative oil production over time. Right: Cumulative CO_2 injection over time. RPT (Relative Permeability Test) represents the relative permeability curves for matrix or fracture system generated by Brooks-Corey equations in CMG simulator (Sorensen et al. 2014). Note that CO_2 injection increased production by 43% to 58%.

Hoffman and Evans (2016) show the first pilot field test results for huff-n-puff in Bakken formation. Even with all the promising results from laboratory tests and simulation results (Son and Yang 2013; Hawthorne et al., 2013 and Sorensen et al., 2014), the field test result failed miserably due containment problems causing early breakthrough and poor reservoir sweep efficiency. Little to no oil rate increase was observed as shown in **Fig. 9**. The solution suggested by authors were employing some type of zonal wellbore isolation or high permeability blocking for containment issues.

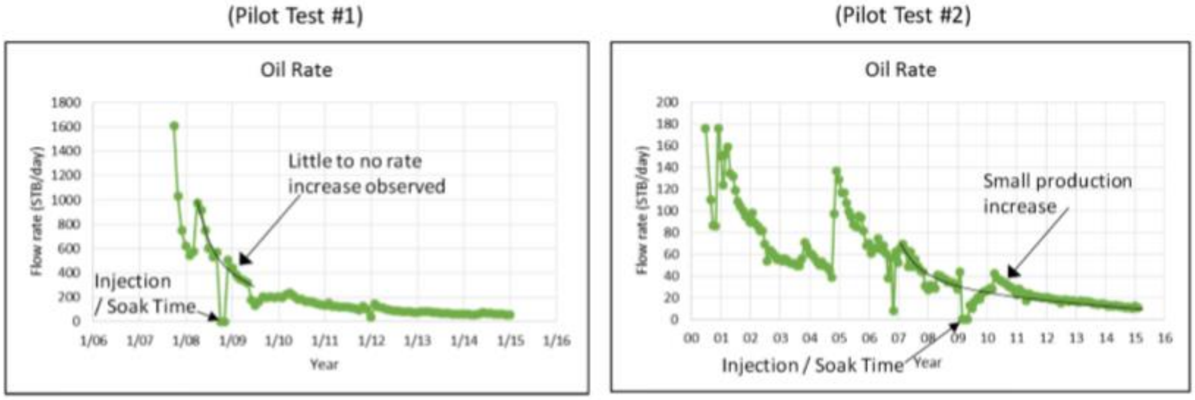

Figure 9: Production from two Bakken wells performing huff-n-puff CO_2 injection. Note that little to no oil rate increase was observed (Hoffman and Evans 2016).

Sorensen et al. (2018) conducted a field study in a vertical well completed in the Middle Bakken formation. The test was conducted in a virgin reservoir without hydraulic fractures to address the problem of containment.. The result of this field study provided valuable lessons; first, even though the injection rate was low, CO_2 can be injected into an unstimulated Middle Bakken reservoir (matrix permeability typically in order of micro to nanodarcies). This supports the findings in the laboratory core tests that solvent gas can permeate into tight rocks during huff-n-puff gas EOR in liquid rich shale. Second, produced fluid composition analysis before injection and after injection indicates that CO_2 mobilized light HCs as shown in **Fig. 10**.

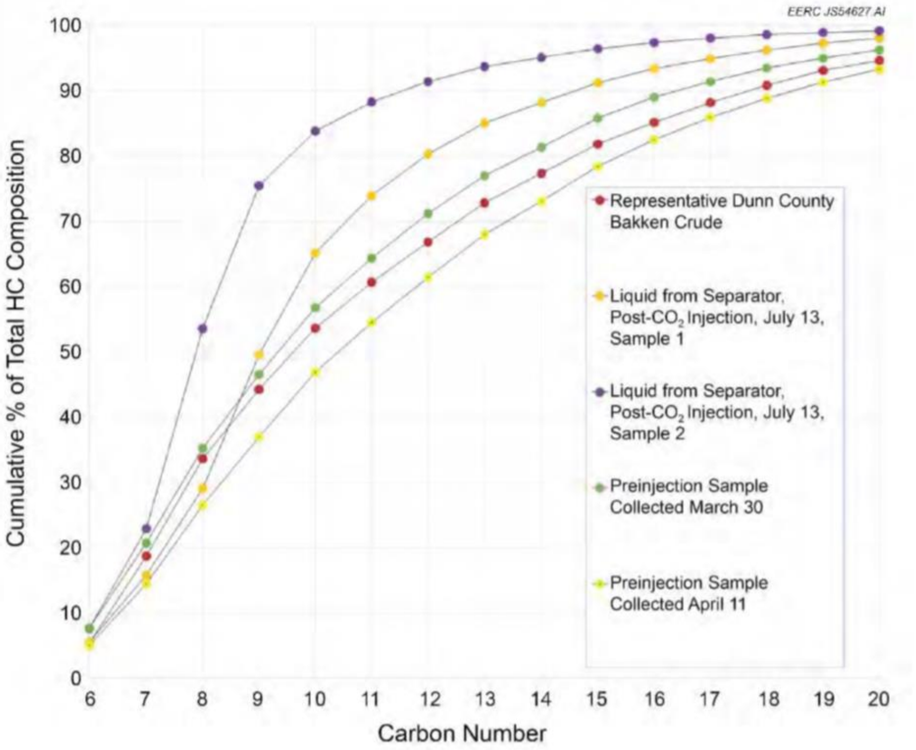

Figure 10: Comparison of pre-injection oil composition, a representative Bakken oil sample and post-injection oil composition. Post-oil composition contains more light HCs (i.e. purple dot has 75% up to C9 where green dot has 75% up to C13) (Sorensen et al. 2018).

Jin et al. (2017) investigated using produced gas for gas injection EOR and to reduce So_x, NO_x, and CO_2 emissions from gas flaring in the Bakken formation. Authors measured MMPs using Vanishing Interfacial Tension (VIT) method of ethane, CO_2, methane and nitrogen in Bakken oil at 230°F: 1344 psi, 2528 psi, 4512 psi, and 14710 psi, respectively. The Middle Bakken samples have a permeability range of 0.008 mD to 0.1 mD and porosity range of 4.0-5.4 %. The effect of gas composition on recovery efficacy of huff-n-puff gas injection was also examined. The results indicate that produced gas performed as well as CO_2 (**Fig. 11**).

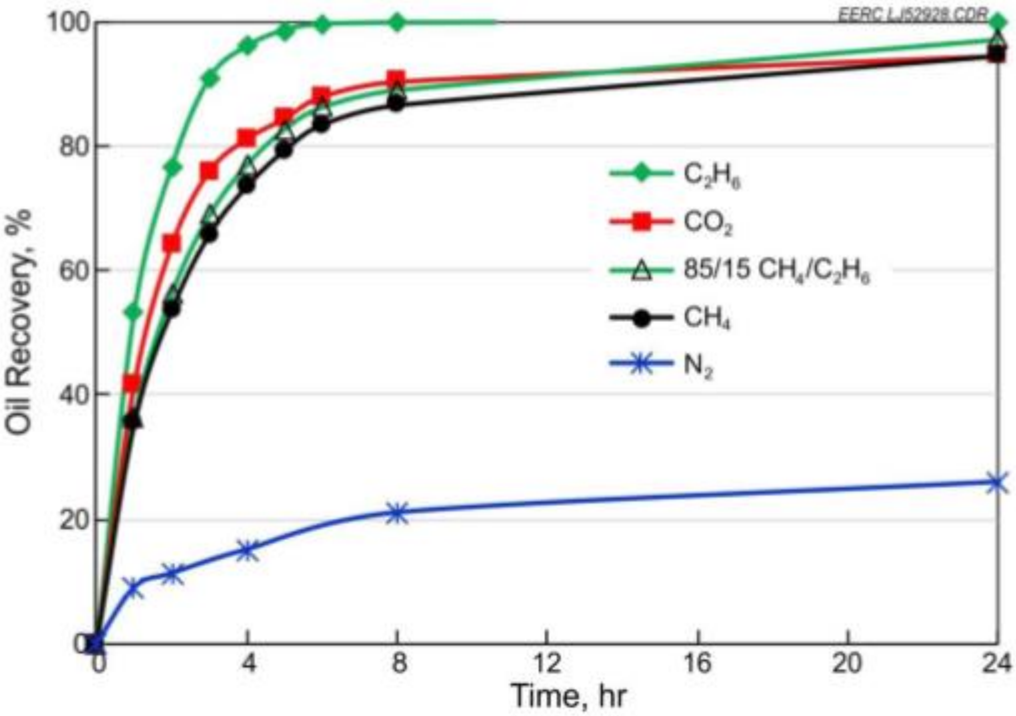

Figure 11: Hydrocarbon recovery from huff-n-puff gas injection EOR using different types of gas for the Middle Bakken samples. Injection pressure was 5000 psi for all the tests. Note that ethane has the highest recovery compared to other gases (Jin et al. 2017).

Yu and Sheng (2016) evaluated the potential of water and N_2 huff-n-puff in Eagle Ford outcrop shale samples (permeability ranged from 300 nD to 500 nD and porosity ranged 8-10%). The samples were saturated with dead oil. Different variables such as soaking time and operating pressure were also investigated. Results show that the potential of water huff-n-puff in shale oil reservoir is limited with a low recovery factor. However, the recovery performance of N_2 huff-n-puff outperformed water huff-n-puff with 10% higher RF, which indicates the positive potential of gas huff-n-puff EOR in Eagle Ford shale. As shown in **Fig. 12**, soaking time did not have a major impact on ultimate recovery factor from N_2 huff-n-puff (i.e. only 7% incremental recovery from 1hr soak to 24 hr soak).

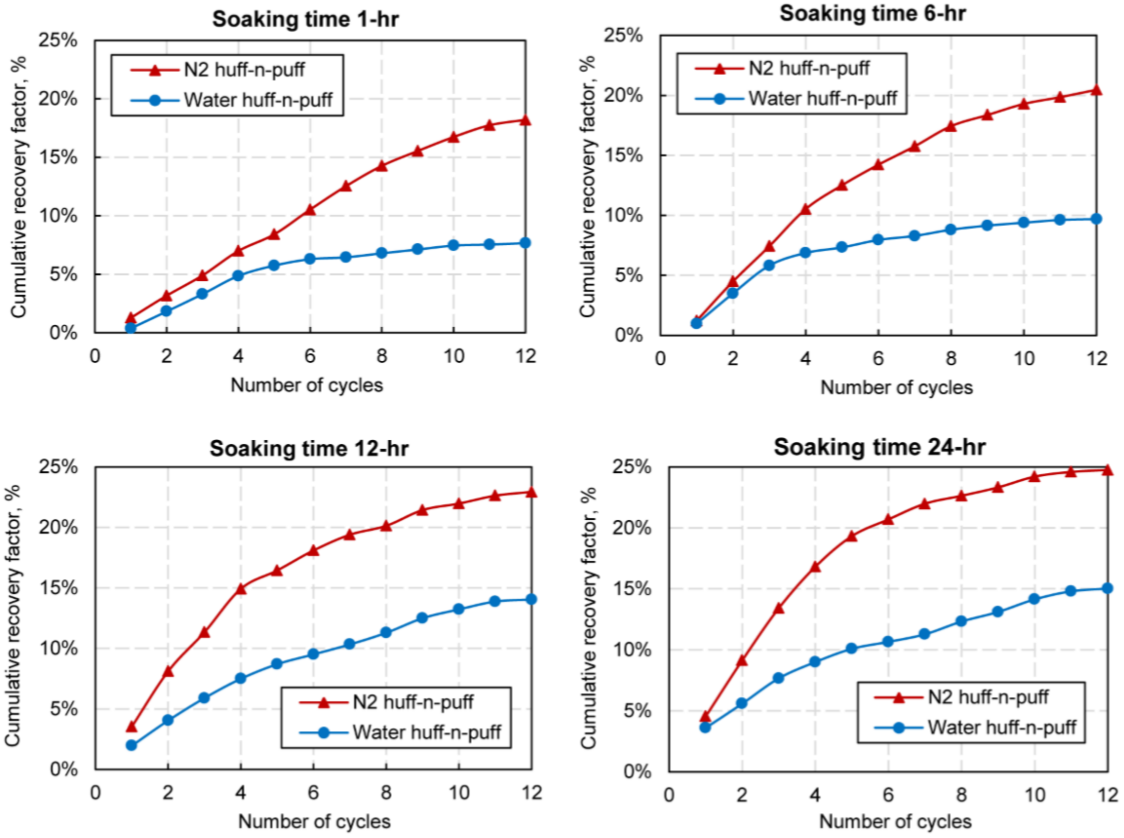

Figure 12: Comparison of recovery efficacy between N_2 and water huff-n-puff with different soaking times. Injection pressure was 1000 psi and temperature was at 72ºF (Yu and Sheng 2016).

Atan et al. (2018) studied the technical and economic viability of gas huff-n-puff in Eagle Ford shale (permeability range of 10 nD-120 nD and 5-8.5% porosity range) using natural gas injection. Compositional simulation models which are calibrated with lab data and history matched for an extended production period were constructed. These models were used to numerically simulate the gas huff-n-puff EOR process and to optimize operating parameters. Simulation results show that stimulated reservoir volume (SRV), containment, and rich gas injectant to be the most important parameters governing the recovery. (**Fig. 13**). Authors also highlight the importance of compressor utilization and commodity price environment

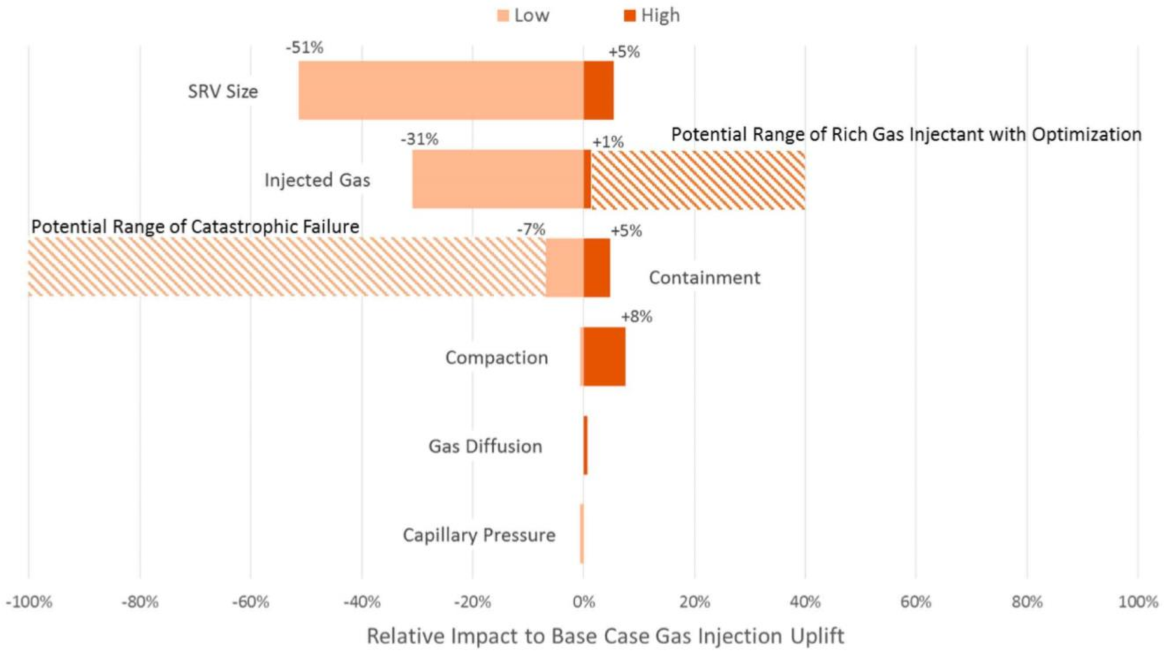

Figure 13: Summary of sensitivity analysis showing the impact of individual parameters. SRV size, rich gas injectant, and containment are three top parameters that impact recovery factor (Atan et al. 2018)

Hoffman (2018) performed forensic analysis of production data of huff-n-puff natural gas EOR pilot wells in Eagle Ford from Texas Railroad Commissions and other sources. Incremental oil recovery was predicted and compared with pre- huff-n-puff forecasts. The results indicated that while some data were hard to interpret because the data are lease based (multiple wells in a lease), for example, there was one lease where all four wells were being injected at the same time.. **Fig. 14** shows the average well oil production rate and lease cumulative oil production and forecasting based on decline curve analysis (DCA). Much valuable information was obtained; first, the initial injection period was roughly 6 months to recharge the reservoirs. Second, injection rate was 2-4 million scf/day and surface injection pressure was around 6000 psi. Third, production period was 2-3 months. Fourth, after the first cycle, injection and soak period was shortened to roughly 2 months. Fifth, this pattern lasted until 4th cycle. After 4th cycle, injection/soaking period was reduced again to 1 month and production period was reduced to 2 months as well. These more frequent cycles yielded additional recovery. The forecasted lease cumulative oil production predicts 50% more oil recovery than the DCA model without huff-n-puff gas EOR process would predict. Overall, the pilots in Eagle Ford were more successful than those in the Bakken.

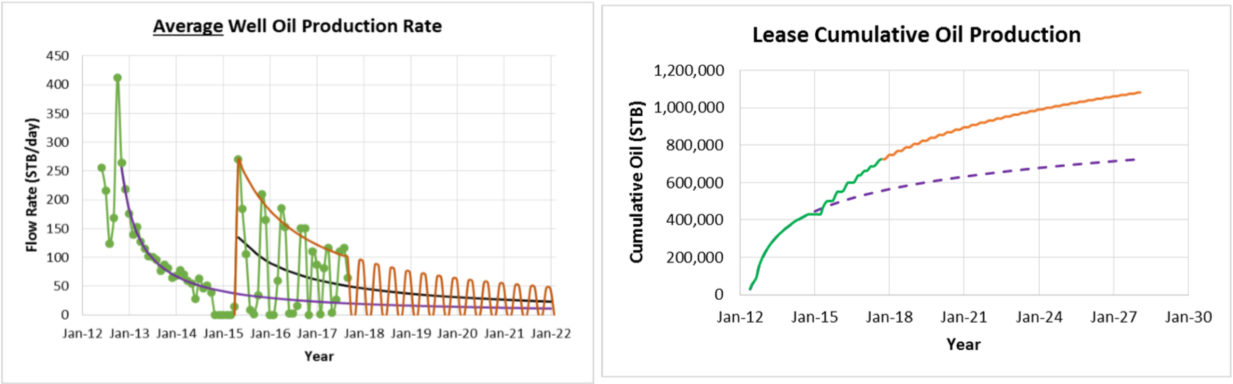

Figure 14: Average well rate and cumulative lease production (in green) and predicted rates and cumulative production (in orange). Purple dashed line indicates that forecasted cumulative oil production based on DCA without huff-n-puff gas EOR process (Hoffman 2018).

Chapter 3: Methodology

3.1 Schematic of experimental setup

The experimental setup for huff-n-puff tests is illustrated in **Fig. 15**. An oven was used to maintain the temperature at 150°F in all experiments. Pressure/temperature sensors are located between the valve and the pressure cell; sensor outputs are fed to a computer. Production flow is regulated using a needle valve to keep production time constant (1 hour).

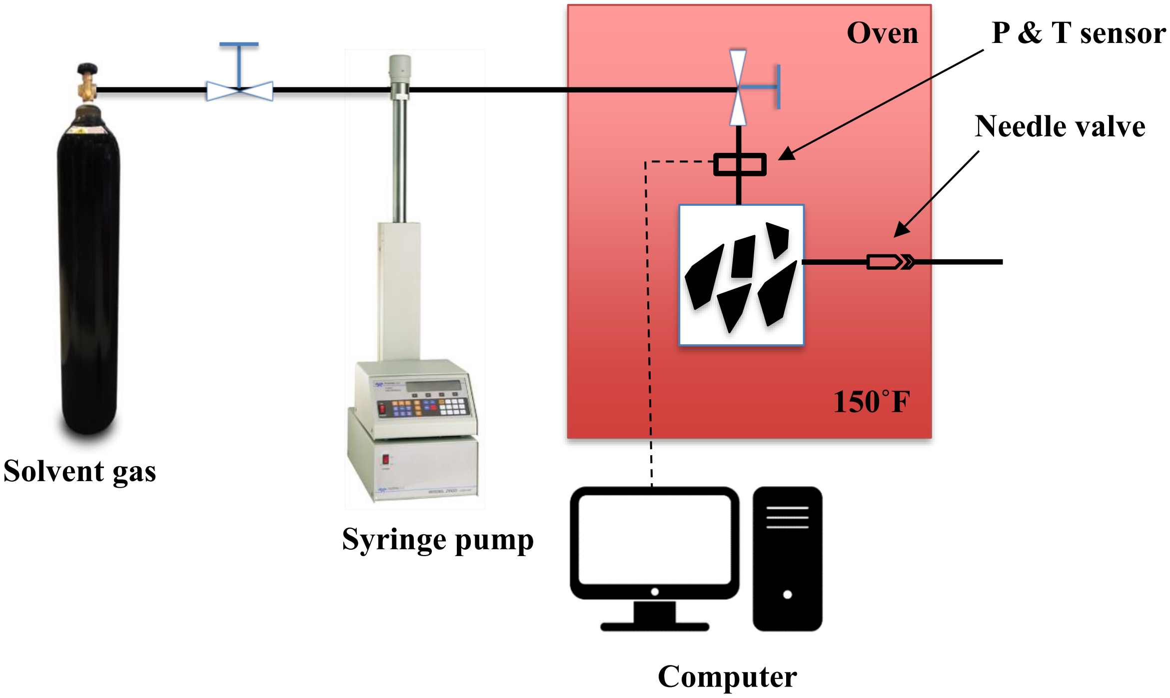

Figure 15: Schematic of experimental setup for a huff-n-puff test. Solvent gas supply is connected to syringe pump. Cuttings are located in the pressure cell within the oven which is heated to 150°F.. Solvent gas is injected at desired pressure and soaked for the prescribed time. Pressure/temperature sensor are connected to and continuously monitored by a computer. After the soaking period, the needle valve is opened to produce for one hour.

3.2 Vanishing Interfacial Tension (VIT) technique

VIT cell is used to measure the MMP of an oil with a solvent gas. VIT cell is an Inferno Sight Feed Indicator (SFI)-6000. It is rated 6000 psi at 100°F.

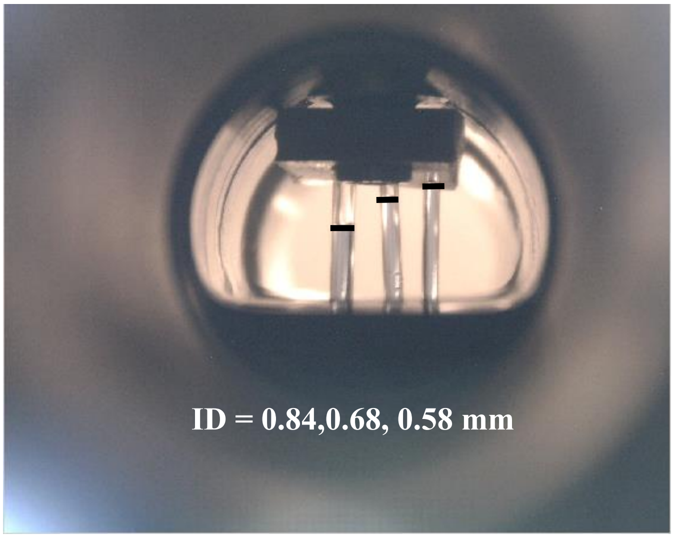

Figure 16: Front view of VIT cell with three different inner diameters capillary tubes; 0.84, 0.68 and 0.58 mm from left to right. Meniscuses are indicated by the black line.

Front view of VIT cell is shown in **Fig. 16**. Three capillary tubes are placed in the cell such that capillary rise of the oil can be observed in the tubes. When solvent gas is injected into the system over a sequence of pressures, the height of meniscus decreases. As injection pressure reaches the MMP value, the height of meniscus essentially becomes the bulk fluid level and disappears. At each pressure step, a picture of the front view of VIT cell is taken to measure the capillary height. The capillary height is measured by measuring pixel distance of image using ImageJ software. In a plot of injection pressure on the y-axis and capillary height on the x-axis, the y-intercept from linear regression gives the value of MMP as shown in **Fig. 17.**

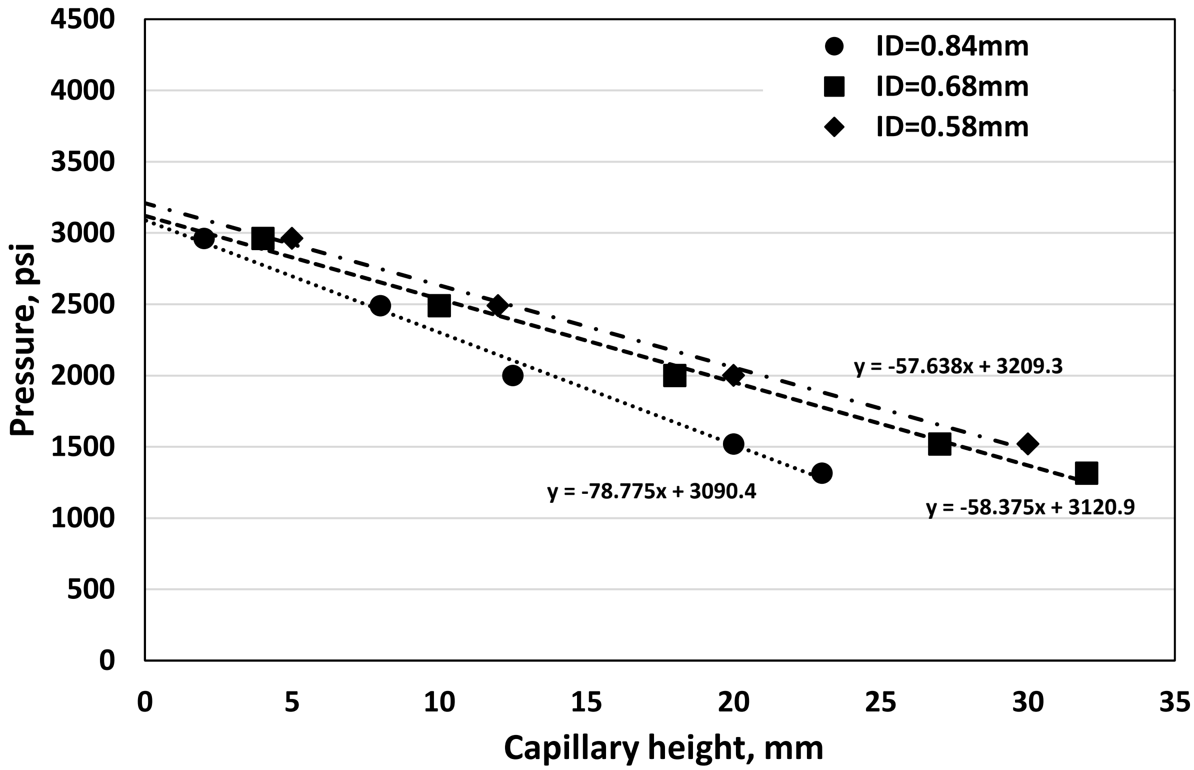

Figure 17: Pressure versus capillary height plot. Solvent gas is mixture of C1:C2 (72:28) and oil is dodecane. Y-intercept of internal diameter (ID) =0.84 mm, 0.68 mm, and 0.58 mm are 3090±61, 3121±68, and 3209±62 psi, respectively. Mean MMP is 3140±64 psi.

3.3 Sample characterization

The petrophysical measurements were done on preserved Eagle Ford shale. These experiments include transmission Fourier Transform Infrared Spectroscopy (FTIR) mineralogy, NMR T_2 relaxation and T1-T2 maps, helium porosity, mercury injection capillary pressure (MICP), HAWK dry pyrolysis analysis, Brunauer-Emmett-Teller (BET) surface area, and LECO™ total organic carbon (TOC).

3.3.1 Petrophysical characterization summary

A summary of petrophysical characterization is shown in **Table 2**, and **Figs. 18 through 22.**

Table 2: Petrophysical properties for Eagle Ford shale sample

Sample	*Total Porosity (%)	TOC (wt%)	Total Clays (wt%)	Total Carbonates (wt%)	Quartz +Feldspar (wt%)	Others
Eagle Ford	**5.1**	**4.9**	**16**	**62**	**13**	**9**

*Total porosity is the summation of NMR porosity and high pressure helium porosimeter (HPP) porosity

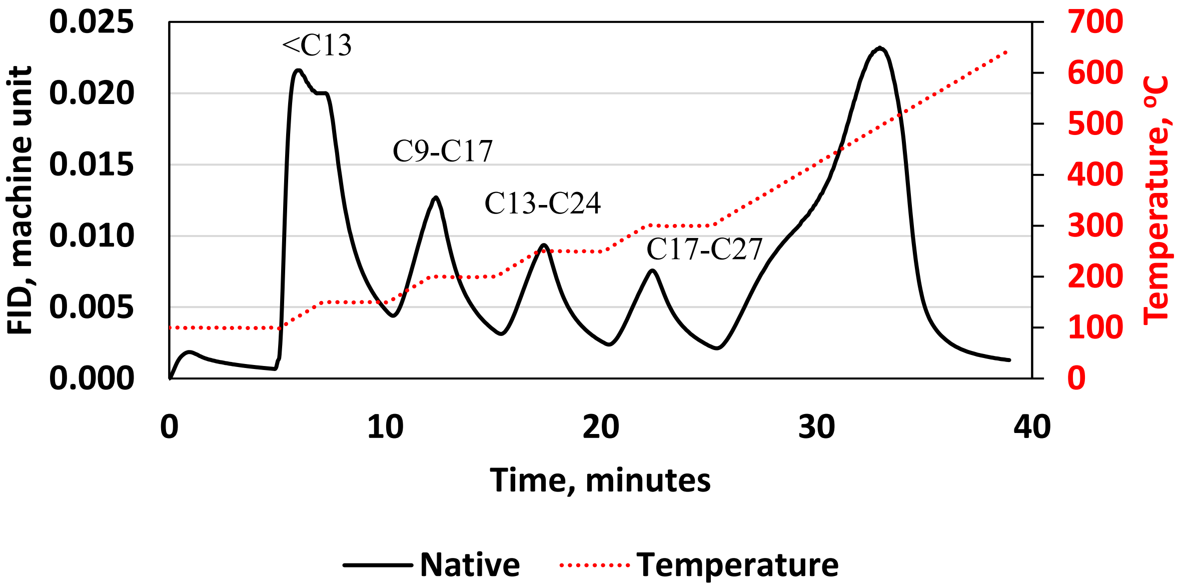

Figure 18: HAWK pyrogram of preserved Eagle Ford sample. First four peaks (S11, S12, S13, and S14) are discrete resolution of the standard S1 peak. The carbon numbers liberated with each peak are indicated. T_{max} (456°C) indicates the thermal maturity of gas condensate. Red curve is the programmed heating.

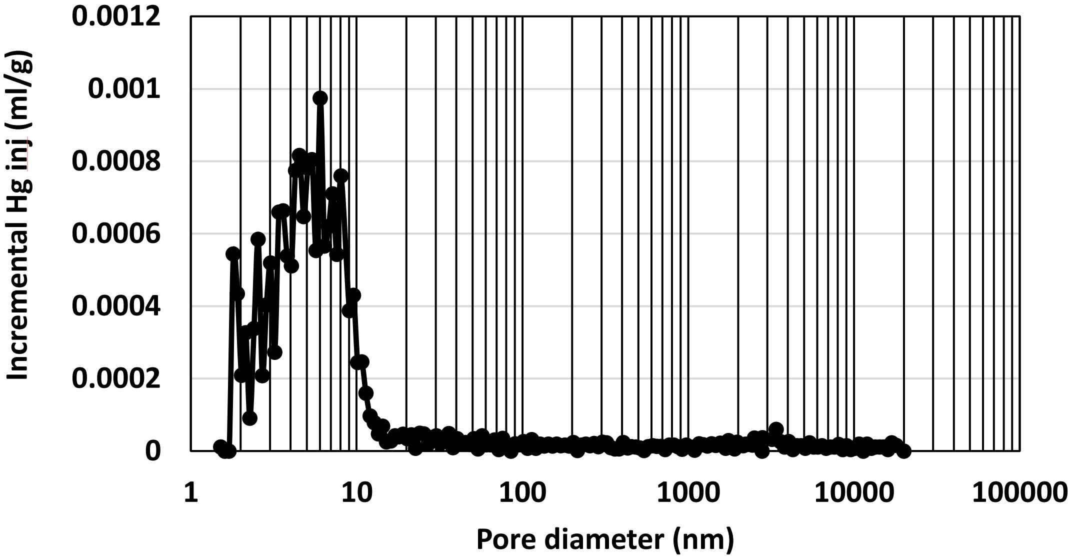

Figure 19: Incremental mercury intake versus pore diameter from MICP of preserved Eagle Ford sample. Most of pore throat sizes are around 6 nm. Gupta (2017) described the MICP technique in detail.

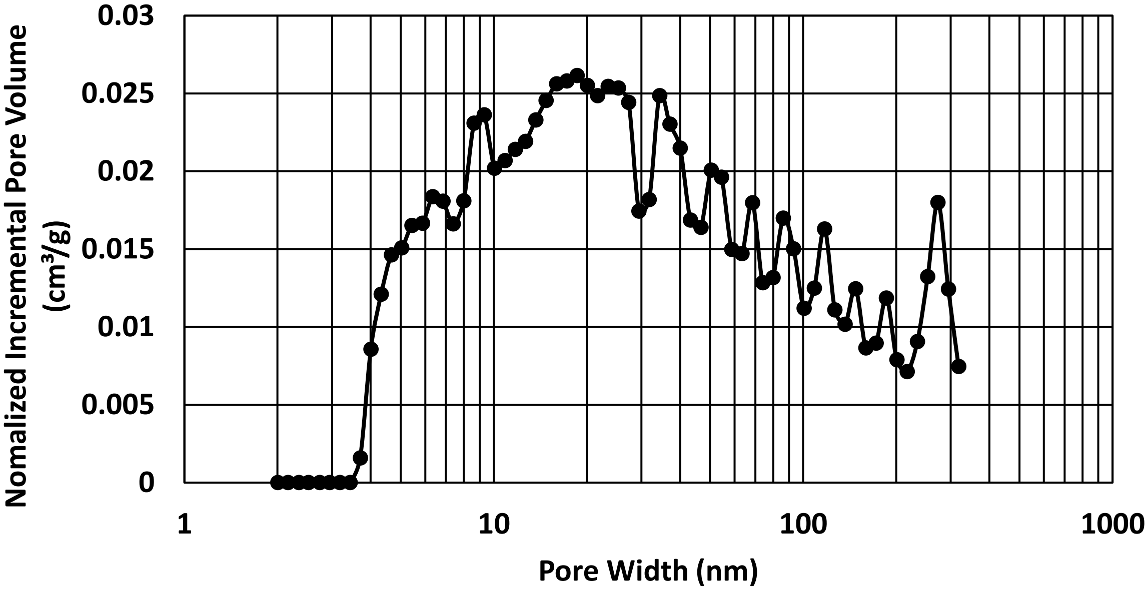

Figure 20: N_2 isothermal adsorption Density Function Theory (DFT) pore size distribution of preserved Eagle Ford sample from BET measurement at -320°F. BET surface area is 1.4 m^2/g. Note that pore size distribution is limited to a maximum of 300nm. Note also that the interpretation is based on pores being slits. Sinha (2017) described the BET technique in detail.

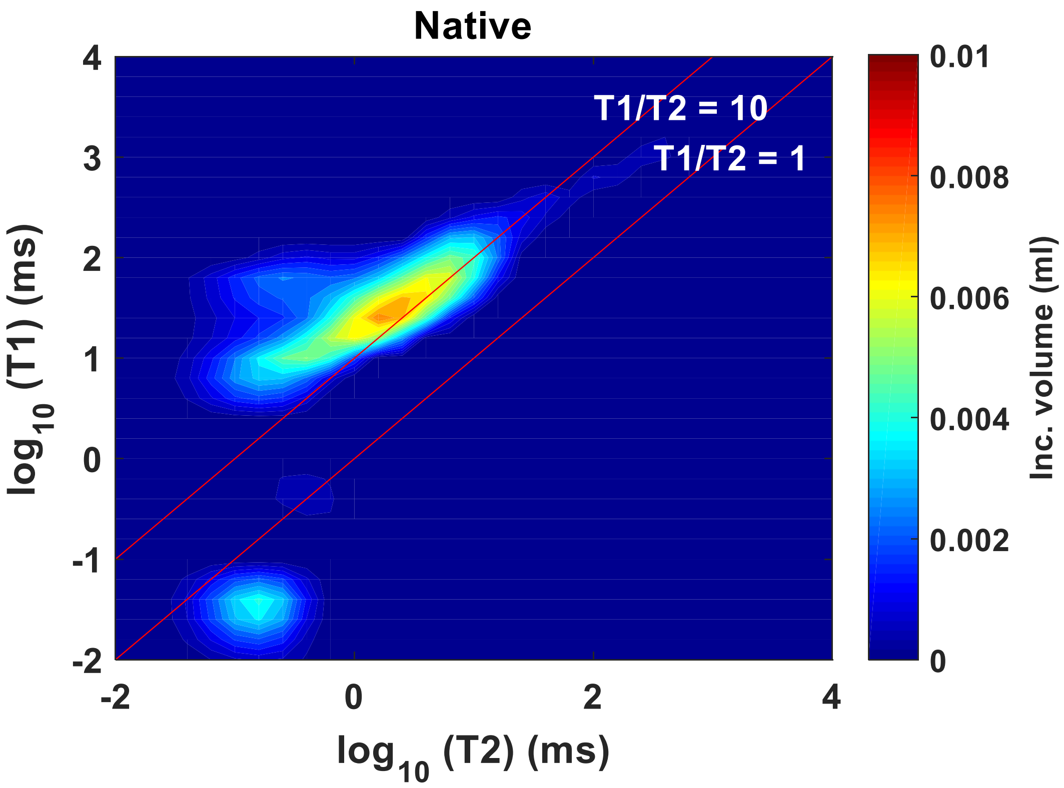

Figure 21: NMR T_1-T_2 map for preserved crushed Eagle Ford sample. T1/T2=10 line represents the oil signal, T1/T2=1 line represents the water signal. Notice that preserved Eagle Ford sample has high oil content compared to water content signal. SNR=73.

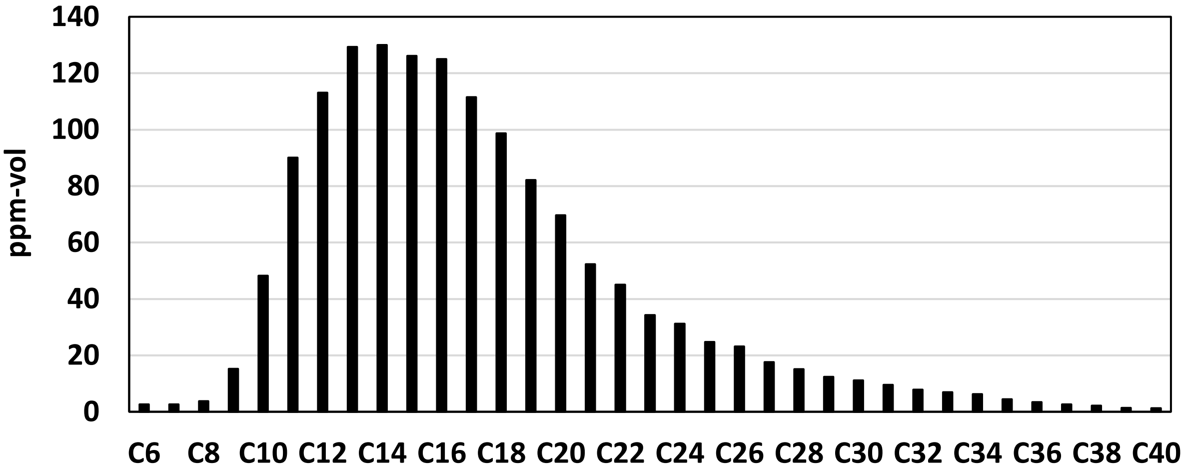

Figure 22: GC analysis of the extracted fluid inside of the preserved crushed rock sample. Note that most of hydrocarbon (HC) number range from C9 to C30.

3.4 Experimental procedures

This section briefly describes sample preparation and experimental protocols. More detailed experimental procedures are documented in **Appendix A.**

3.4.1 Sample preparation

The samples used in this experiment are from the lower Eagle Ford shale. Cores are preserved and cut dry. A portion of the sample was crushed. Sieves were used to select a sample size between 6.7-8mm. These tests on crushed samples are referred to "coffee bean" test in this study (**Fig. 23**). This coffee bean size was chosen as an optimal size for quick screening for huff-n-puff tests. This sample size is small enough that it does not require longer soaking time but large enough to preserve the micropore structure. After crushing, samples are stored in glass vials wrapped with plastic wrap, aluminum foil, and finally parafilm to prevent the loss of fluids in preserved samples between the cycles.

Figure 23: Crushed sample (6.7-8mm) from Eagle Ford sample.

3.4.2 Experiment protocols

T_2 and T_1-T_2 measurements were done in 12 MHz Oxford GeoSpec2 NMR spectrometers using Green Imaging™ software for acquisition and processing. Operating parameters for NMR measurement are shown in **Table 3**.

Table 3: Operating parameters for T_2 and T_1-T_2 measurements

	Time/Number of scans (NSA)	Tau, (μs)	T_2 max, (ms)	T_1 max, (ms)
T_2	Time=8 minutes	57	100	
T_1/T_2	NSA=32	57	100	200

After the NMR test, crushed samples are placed in high pressure cell. This cell is placed in the oven until temperature equilibrium is reached (150°F). Solvent gas is injected at the rate of 30cc/min to achieve the injection pressure and then soaked (huff phase). With this injection rate the injection pressure was achieved within 5 minutes. After the desired amount of soaking time, pressure is released through needle valve (puff phase) for one hour. Samples are taken out from the cell and cooled to room temperature in a desiccator. T_2 and T_1-T_2 measurement are performed again to measure the change of fluids in a shale sample during huff-n-puff EOR. This process is repeated until recovery reaches a plateau. Note that each NMR T_2 test is for 8 minutes, which is equivalent to 352 NSA. Therefore, Signal to Noise Ratio (SNR) will decrease as cycle proceeds (producing fluids). This leads the increase in inherent NMR error in each cycle.

Chapter 4: Results and discussion

4.1 Minimum Miscibility Pressure (MMP) measurements by Vanishing Interfacial Tension techniques (VIT)

MMP was measured using a VIT method (Hawthorne et al. 2014). **Fig. 24** shows plots of pressure versus capillary height for a methane-dodecane system. Linear regression is used to find y-intercept which represents the capillary height of zero. MMP is defined as the pressure at which the interfacial tension between the injected fluid and crude oil phases decreases to zero (Rao and Lee, 2000). The rise in a capillary tube is governed by Eqn. 1

$$h = \frac{2\gamma \mathrm{Cos}\theta}{\Delta\rho g r} \qquad \ldots\ldots\ldots\ldots\ldots\ldots\ldots (1)$$

Where,

h: height of the capillary rise, cm

γ: interfacial tension, dyne/cm

θ: contact angle of the liquid on the capillary material, degrees

r: radius of capillary tube, cm

$\Delta\rho$: difference between density of the two immiscible phases, g/cc

g: gravity, cm/s^2

When interfacial tension is zero, the height in capillary tube is also zero. MMP is the y-intercept value of pressure versus capillary height plot. MMP between dodecane and methane was found to be 4156±103 psi. This value compares favorably with the results from the multiple mixing cell method in WinProp (CMG software) which yields a value of 4116 psi.

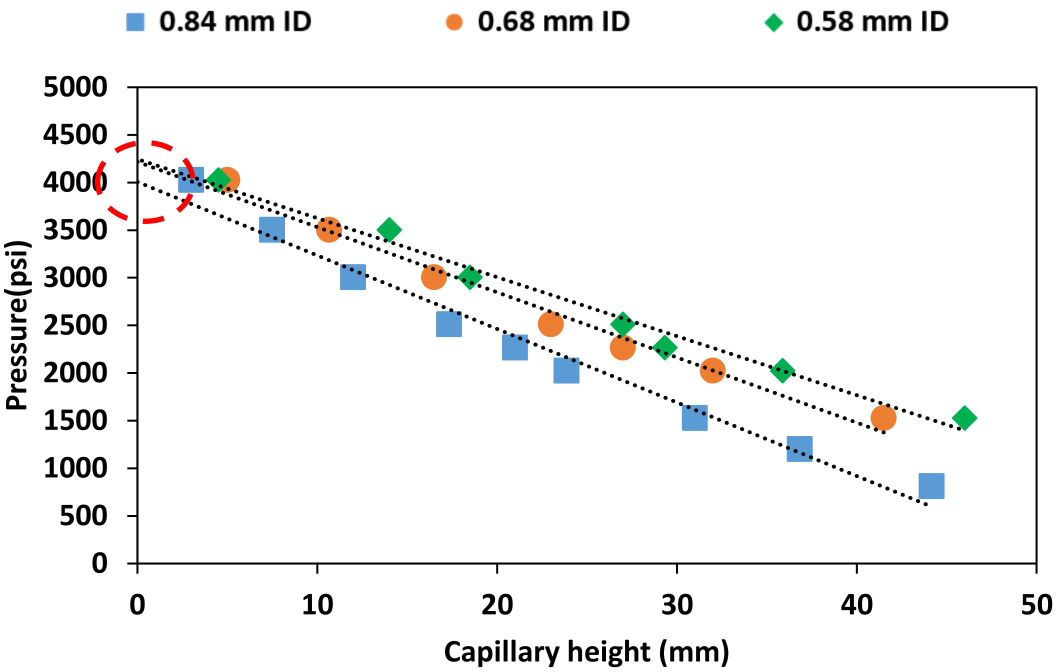

Figure 24: Pressure versus capillary height. Solvent gas is methane and oil is dodecane. Y-intercepts for capillary tube diameters of (ID) of 0.84mm, 0.68mm, and 0.58mm are 4007±106, 4217±104, and 4245±100 psi, respectively. Mean MMP is 4156±103 psi.

Fig. 25 shows the pressure versus capillary height plot for methane-Eagle Ford oil system. Nonlinear behavior was observed above 3000 psi. This behavior is due to the nonlinear density behavior of methane when pressure exceeds 3500 psi as shown in **Fig. 26**. In order to mitigate non-linear behavior in pressure vs capillary plot, the pressure is converted to the density using **Fig. 26**. **Fig. 27** shows density versus capillary height plot of methane-Eagle Ford oil system. This improved the linear regression fit; calculation of MMP in pressure space yields a value of 5391±335 psi while in density space yields a value of 5890±190 psi. Standard deviation of the MMP value in density space is 56% of standard deviation of the MMP value in pressure space.

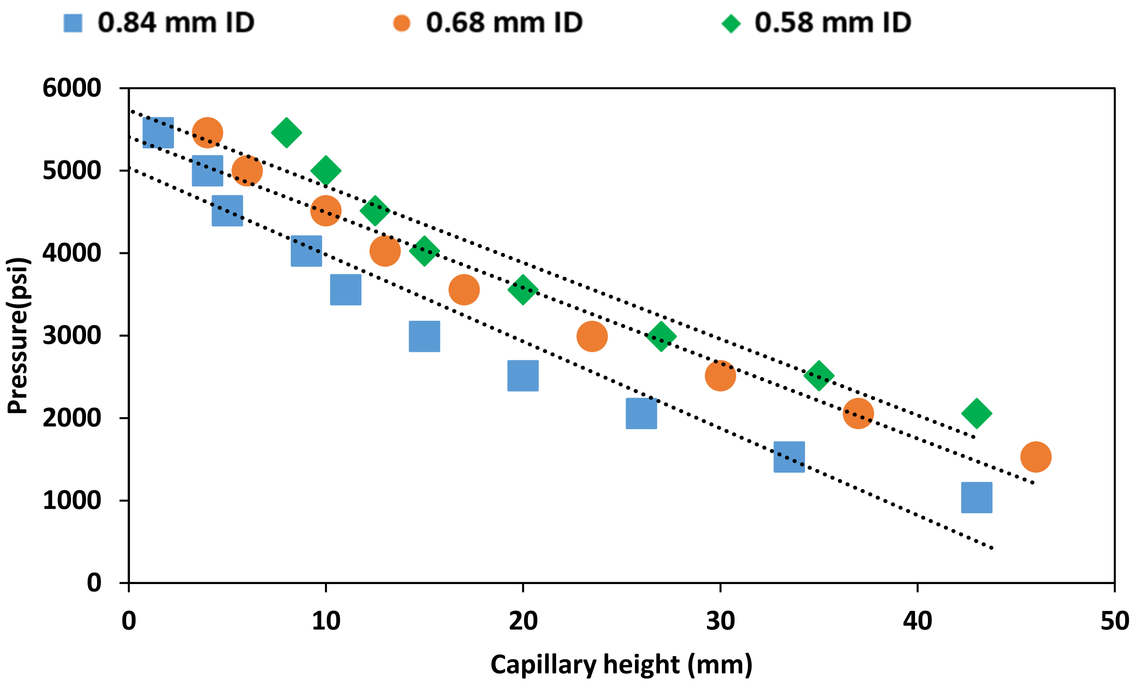

Figure 25: Pressure versus capillary height plot for three capillary tubes having diameters of 0.58 mm, 0.68mm and 0.84mm. Solvent gas is methane and oil is Eagle Ford oil. Y-intercepts of the best fitting lines are 5035±209, 5408±152, and 5733±100 psi, respectively. Mean MMP is 5391±335 psi.

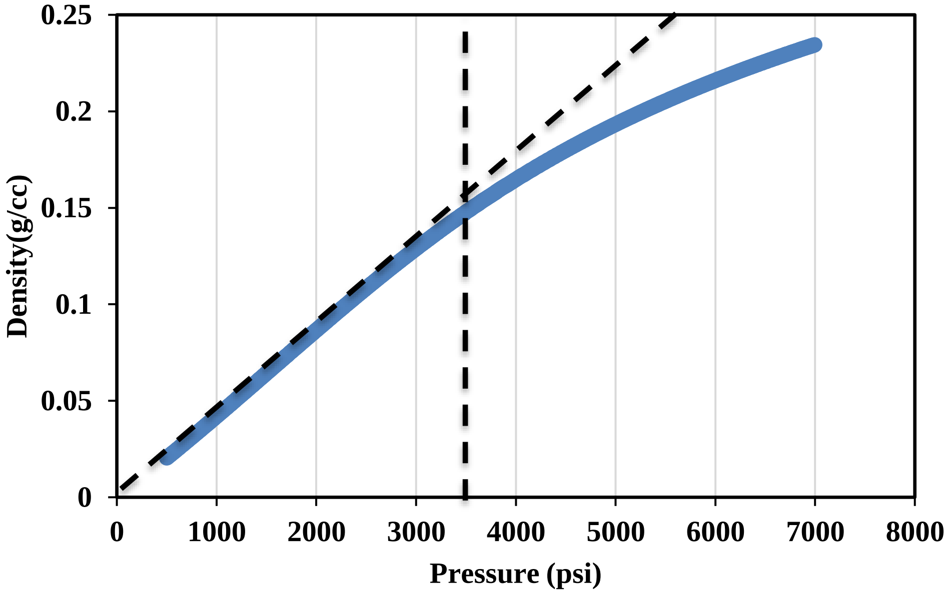

Figure 26: Density versus pressure plot of methane generated from National Institute of Standards and Technology (NIST) software. Notice that after 3500 psi, there is deviation from linear behavior

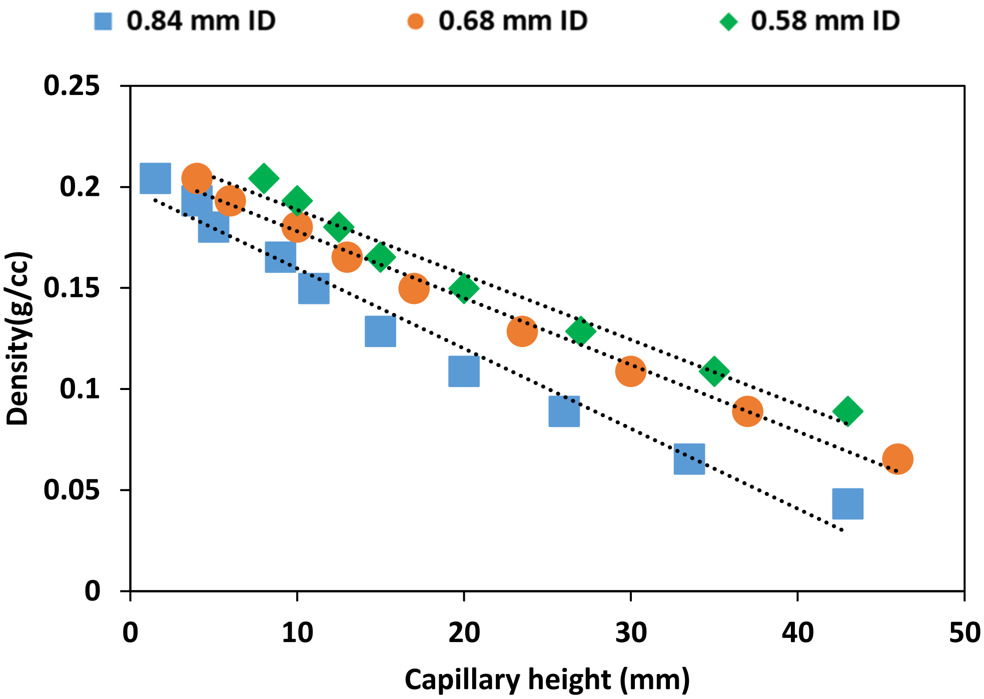

.

Figure 27: Density versus capillary height plot for the same data as in Fig 26 but now corrected for the nonlinear density-pressure dependence. Solvent gas is methane and oil is Eagle Ford oil. Notice that after pressure is converted to density, it exhibits more linear behavior. Mean MMP value is 5890±190 psi.

Different solvent gases were used for MMP measurements. **Fig. 28** shows the summary of all the MMP measurements in this study. Methane showed the highest MMP value followed by the mixture C1:C2 (72:28), field gas and ethane with the two different oils used in this study. **Table 4** gives the composition of the field gas.

Table 4: Composition of the produced field gas analyzed by GC chromatography

Alkane	Mole %
C1	75.76
C2	13.06
C3	7.05
C4	2.95
C5-C8	1.19

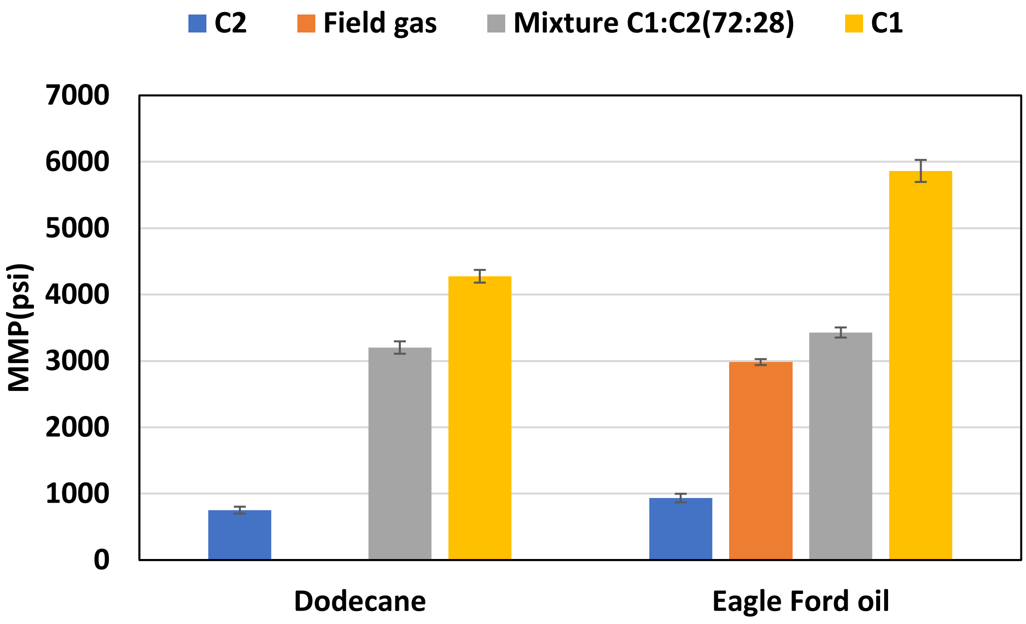

Figure 28: Summary of all the MMP measurements from the study. Note that as methane composition in solvent gas increases, the MMP value increases for the same oil.

4.2 Impact of soaking time for huff-n-puff EOR

Table 5 shows the matrix of the soaking experiments.

Table 5: Matrix of soaking experiments. Preserved sample sizes were 6.7-8mm and the amount of sample used for each experiment was about 22 grams and the same gas composition was used. Production time for all the tests was one hour.

Crushed sample tests				
Test #	**Soak Time(hr)**	**# Cycle**	**Gas**	**Pressure(psi)**
1	1	12	Mixed gas C1:C2 (72:28)	4500
2	3	10	Mixed gas C1:C2 (72:28)	4500
3	6	4	Mixed gas C1:C2 (72:28)	4500

Fig. 29 shows successive NMR T_2 spectra of the remaining fluid in the Eagle Ford sample after test 1. Green triangles represent the preserved state of the sample. Faster T_2 relaxation region (0.01ms to 1ms) represents small pores or heavy fluids or strong affinity fluids (i.e. oil resides in

strongly oil wet pores). Slower T_2 relaxation region (1ms to 30ms) represents large pores or light fluids or weak affinity fluids. Cycle 1 represents the state of the sample after 1 cycle of huff-n-puff EOR. As huff-n-puff cycles proceed from base to cycle 12, there are reductions in T_2 amplitudes not only from slower T_2 relaxation region (i.e. light hydrocarbon or fluid in big pores) but also from faster T_2 relaxation region (i.e. heavy hydrocarbon or fluid in small pores). However, most of production comes from the slower T_2 relaxation region (1ms to 30ms), implying from fluids in larger pores or light hydrocabons

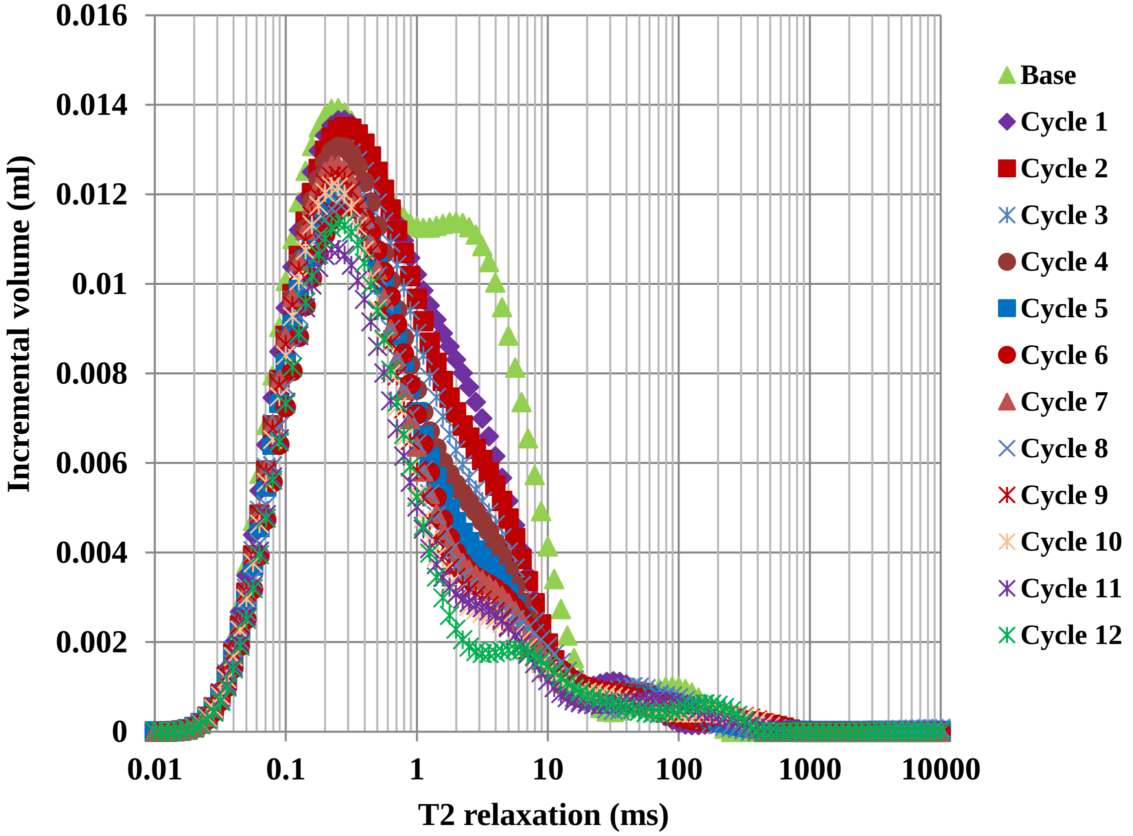

Figure 29: Successive (12 MHz) T_2 spectra of test 1 (12 cycles with one hour soaking time. Mixed gas C1:C2 (72:28) was injected at 4500 psi, which is 1000 psi above MMP). Note that NMR volumes between T_2 relaxation regions of 1ms to 30ms are preferentially decreasing. This indicates that light hydrocarbon or fluid in bigger pores is produced during the huff-n-puff.

Fig. 30 is the cumulative recovery plot of test 1. Recovery was calculated from T_2 NMR data. First cycle recovery is the greatest recovery of all cycles. Ultimate recovery of test 1 at the end of 12 cycles is 45%. It is worth noting that around cycle 6, recovery is plateaued; after that, recovery started to increase again. This might indicate possiblity of cleanning small pores which provides access to larger pores for solvent gas to enter.

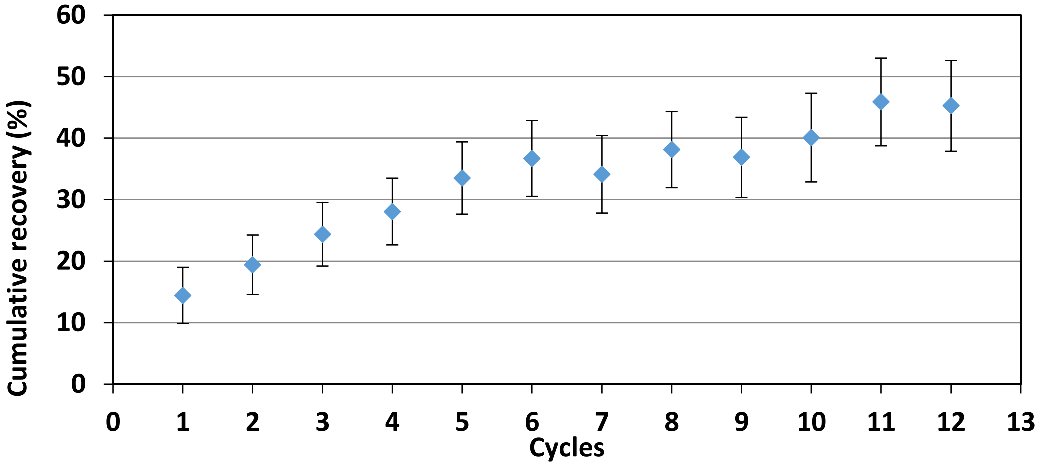

Figure 30: Cumulative recovery versus cycles of test 1 (12 cycles with one hour soaking time. Mixed gas C1:C2 (72:28) was injected at 4500 psi, which is 1000 psi above MMP). Ultimate recovery is 45%. Note that each error bar increases as cycle proceeds, this is due to the fact that as NMR volume decreases, the inherent NMR error increases.

Both test 2 and test 3 NMR T_2 spectra and recovery results are shown in **Figs. 31** through **34.** NMR T_2 spectra for both test 2 and test 3 exhibit similar behavior to test 1, which shows most reduction in T_2 amplitude in slow T_2 region (1ms to 30ms). Also, the first cycle yields the highest recovery of all cycles in both test 2 and test 3. This behavior has been observed in many experimental works (Hawthorne et al., 2013; Gamadi et al., 2013; Li and Sheng, 2016; Yu, 2016 and Zhang et al., 2018**)**. Rognmo et al. (2017) explained that this behavior is an indication of molecular diffusion mechanism becoming the more dominant mechanism over time.

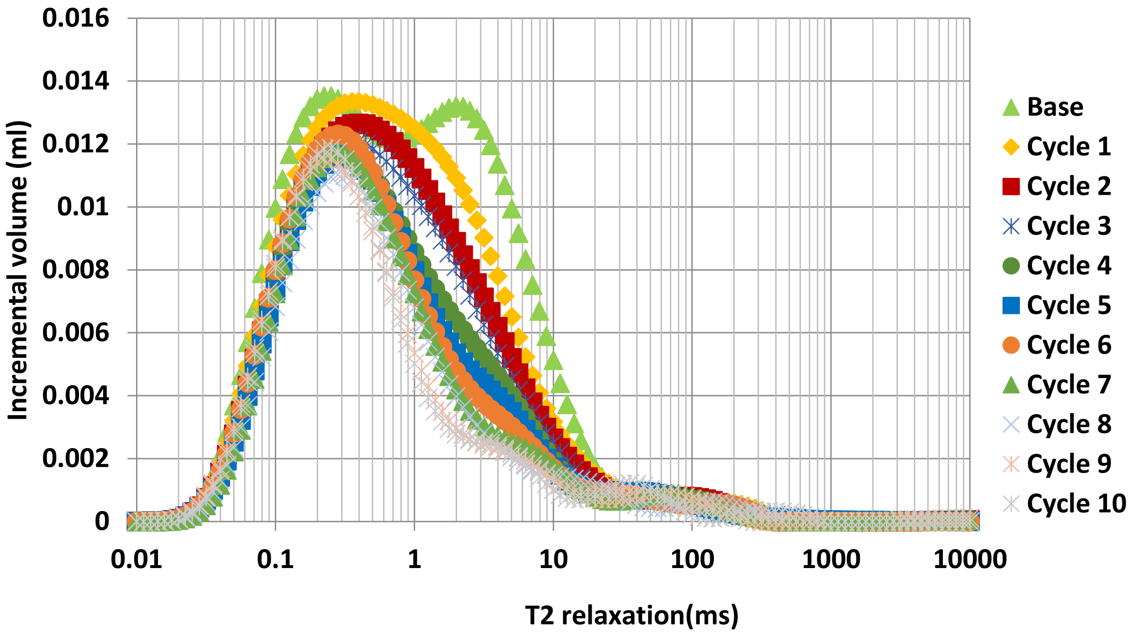

Figure 31: Successive T_2 spectra of test 2 (10 cycles with three hour soaking time. Mixed gas C1:C2 (72:28) was injected at 4500 psi, which is 1000 psi above MMP). Note that NMR volumes between T_2 relaxation regions of 1ms to 30ms are preferentially decreasing. This indicates that light hydrocarbon or fluid in bigger pores is produced during the huff-n-puff.

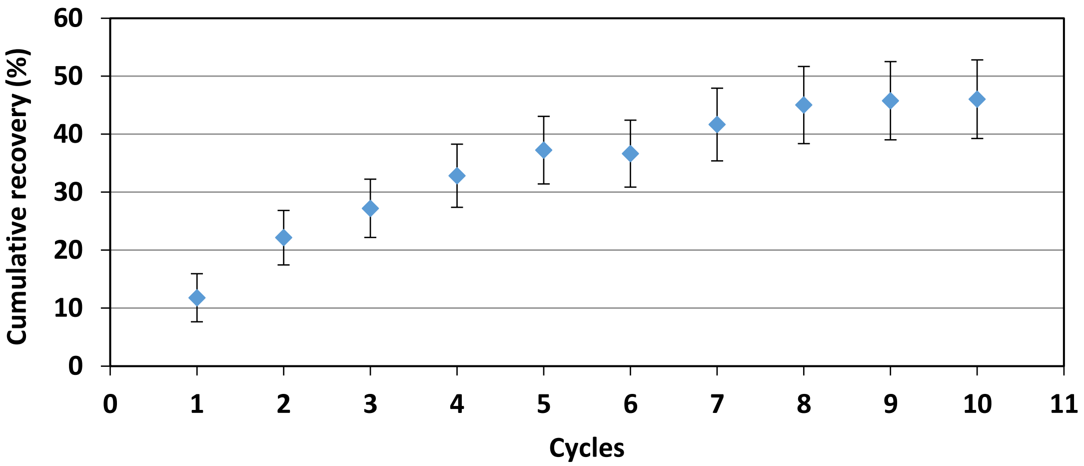

Figure 32: Cumulative recovery versus cycles of test 2 (10 cycles with three hour soaking time. Mixed gas C1:C2 (72:28) was injected at 4500 psi, which is 1000 psi above MMP). Ultimate recovery is 46%. Note that each error bar increases as cycle proceeds, this is due to the fact that as NMR volume decrease, the inherent NMR error increases.

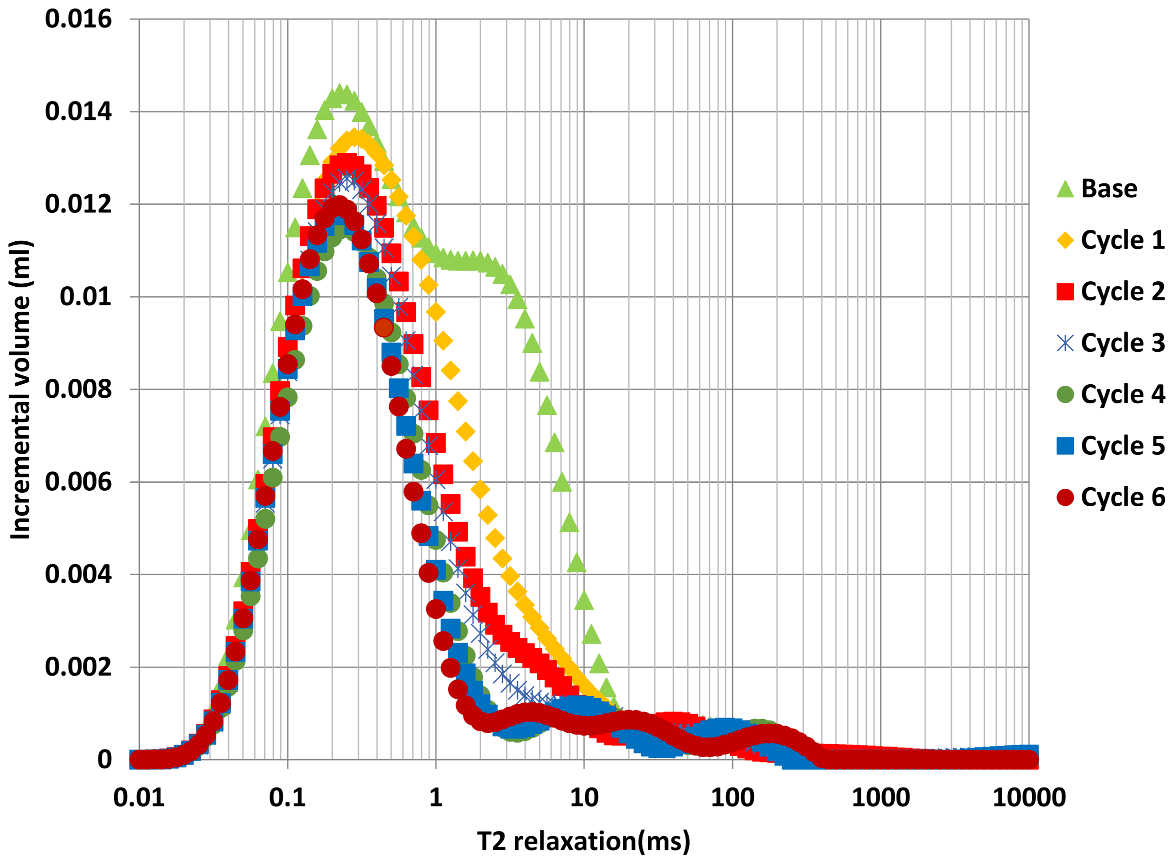

Figure 33: Successive T_2 spectra of test 3 (6 cycles with six hour soaking time. Mixed gas C1:C2 (72:28) was injected at 4500 psi, which is 1000 psi above MMP). Note that NMR volumes between T_2 relaxation regions of 1ms to 30ms are preferentially decreasing. This indicates that light hydrocarbon or fluid in bigger pores is produced during the huff-n-puff.

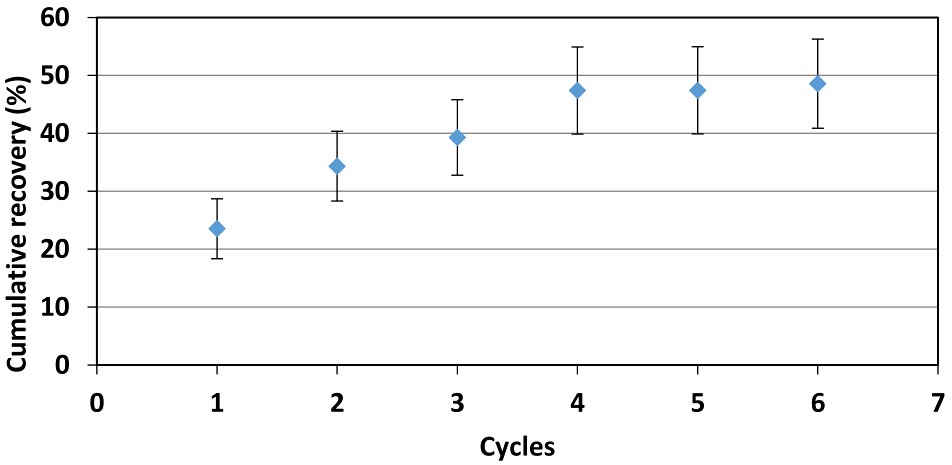

Figure 34: Cumulative recovery versus cycles of test 3 (6 cycles with six hour soaking time. Mixed gas C1:C2 (72:28) was injected at 4500 psi, which is 1000 psi above MMP). Ultimate recovery is 49%. Note that each error bar increases as cycle proceeds, this is due to the fact that as NMR volume decrease, the inherent NMR error increases.

Recovery result from all the tests are summarized in Fig. 35. Ultimate recovery at the end of the experiments are 45%, 46%, and 48% for 1hr soak, 3hr soak, and 6hr soak time, respectively. These recoveries are very similar. However, the 6hr soak shows the highest recovery in cycle 5 compared to the 3hr and 1hr soaks. This seems that longer soaking time will yield higher recovery. However, this is misleading since the x-axis is just the number of cycles performed. **Fig. 36** is the similar recovery summary plot, but with different x-axis, viz. residence time. Residence time is defined as effective average length of time that a gas molecule, will remain contact with the shale sample in the pressure cell. In this study, residence time is simply the summation of soaking time and production time. It is important to include production time because gas molecules are still in contact with the sample during the production time. Since the production time for all experiments was 1hr. Residence times for each cycle for 1hr soak, 3hr soak, and 6hr soak are 2hr, 4hr, and 7hr, respectively. **Fig. 36** shows when recovery is a function of residence time, it does not matter if soaking time is longer or shorter. Provided that the residence time is same, even with different number of cycles, the recovery is similar. Simple economic analyses were performed using a strategy of longer soaking time with lower number of cycles or shorter soaking with a greater number of cycles. In the case of this study, simple profit/hr ratio was calculated assuming an oil price of \$65/bbl and a gas price of \$2.5/MCF. The result is shown in **Fig. 37**. Six hour soak has the highest profit/hr ratio due to the fact that with a smaller number of cycles, the cost of gas injected was cheaper compared to the shorter soaking time with a greater number of cycles.

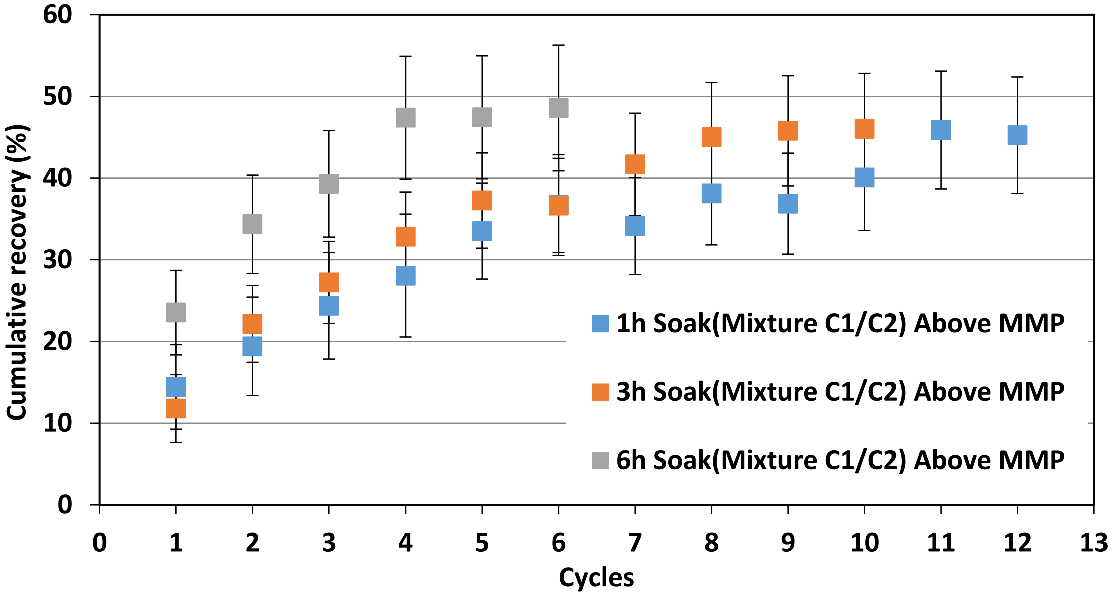

Figure 35: Summary of recovery versus cycles from three different soaking times at 1000 psi above MMP. Final recovery at the end of each experiment are 45%, 46%, and 49% for 1hr, 3hr, and 6hr soaking times, respectively.

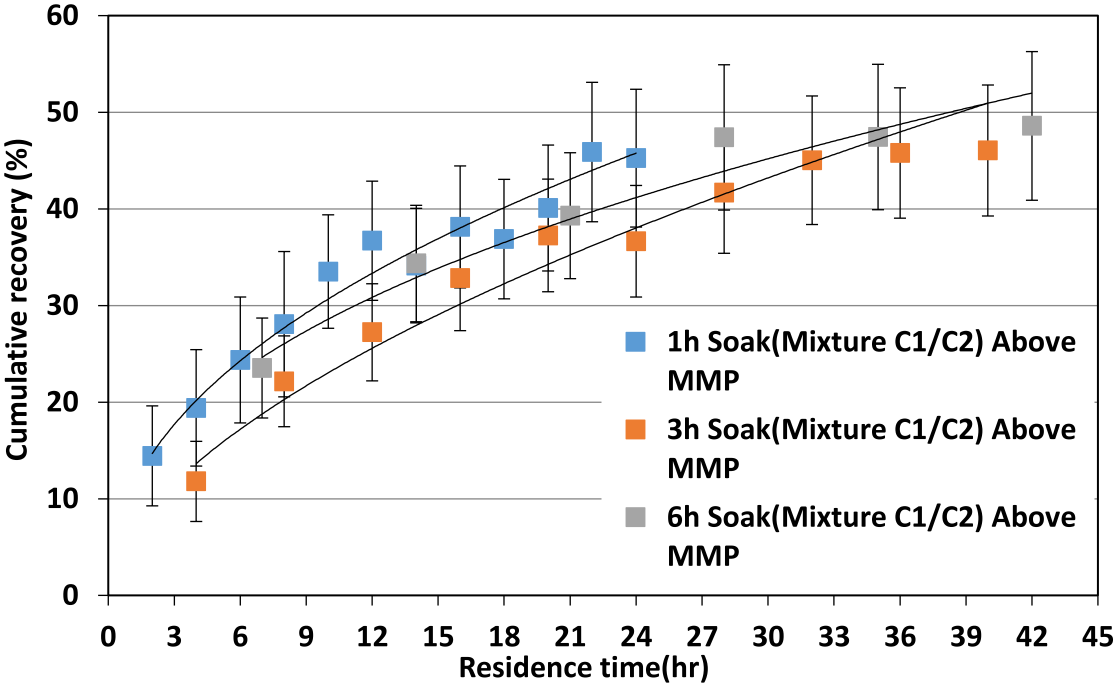

Figure 36: Summary of recovery versus residence time from three different soaking times at 1000 psi above MMP. Residence time is the sum of soaking time and production time. It is worth noting that at the same residence time, recovery is very similar regardless of soaking time.

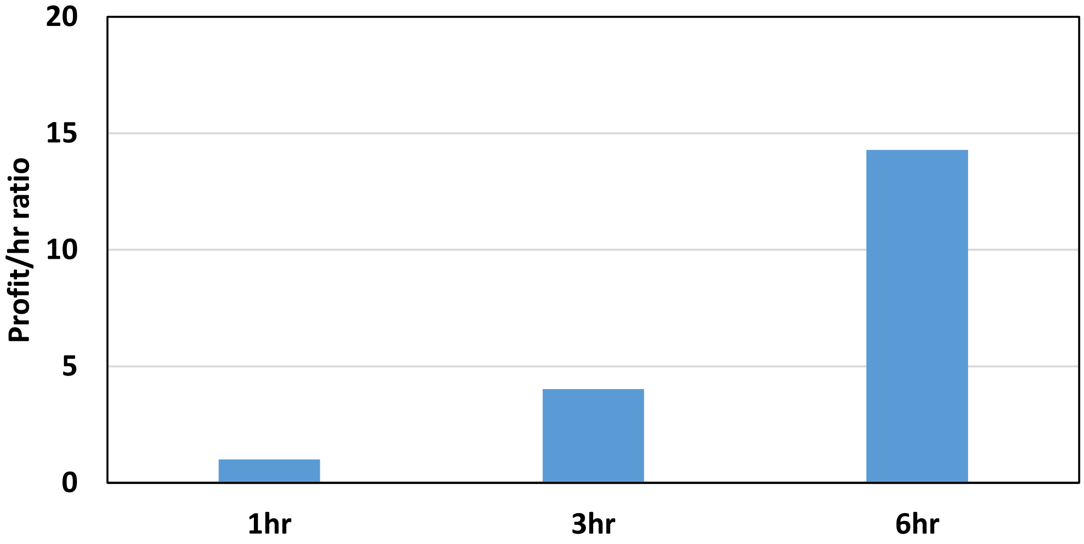

Figure 37: Profit/hr ratio versus soaking time. Profit/hr ratio was calculated assuming an oil price of $65/bbl and a gas price $2.5/mcf.

To investigate the produced fluid composition, HAWK pyrolysis analysis and GCMS analysis were performed on crushed samples after huff-n-puff EOR. **Fig. 38** shows the pyrograms of HAWK analysis. The HAWK is a programmable dry pyrolysis instrument; it can break down the S1 signals to into four different fractions; S11, S12, S13, and S14. Each S1x signal represents a temperature fractionation of <C13, C9-C17, C13-C24, and C17-C27, respectively (Abrams et al. 2017). **Fig. 39** is the S1 fraction summary of HAWK analysis with respect to soaking time. All pyrograms have the recoveries only up to S13, i.e. the C13-C24 hydrocarbons. S14 signal does not exhibit any significant change. **Fig. 40** and **Fig. 41** shows the results of GC analyses on residual rock with respect to soaking time. Hydrocarbons produced are mostly up to C25 for all three soaking time. The GC analysis confirmed the HAWK pyrolysis analyses. It also confirmed that longer soaking time, 6hr, can produce slightly heavier hydrocarbons (**Fig. 41**). It is worth noting that produced HCs are preferentially lighter hydrocarbons. First, this is due to that lighter hydrocarbons has lower viscosity, hence has higher mobility. Second, as like dissolves like states

it, lighter hydrocarbon has similar polarity with injected C1/C2 (light hydrocarbons) polarity. Hence, lighter hydrocarbons dissolves better.

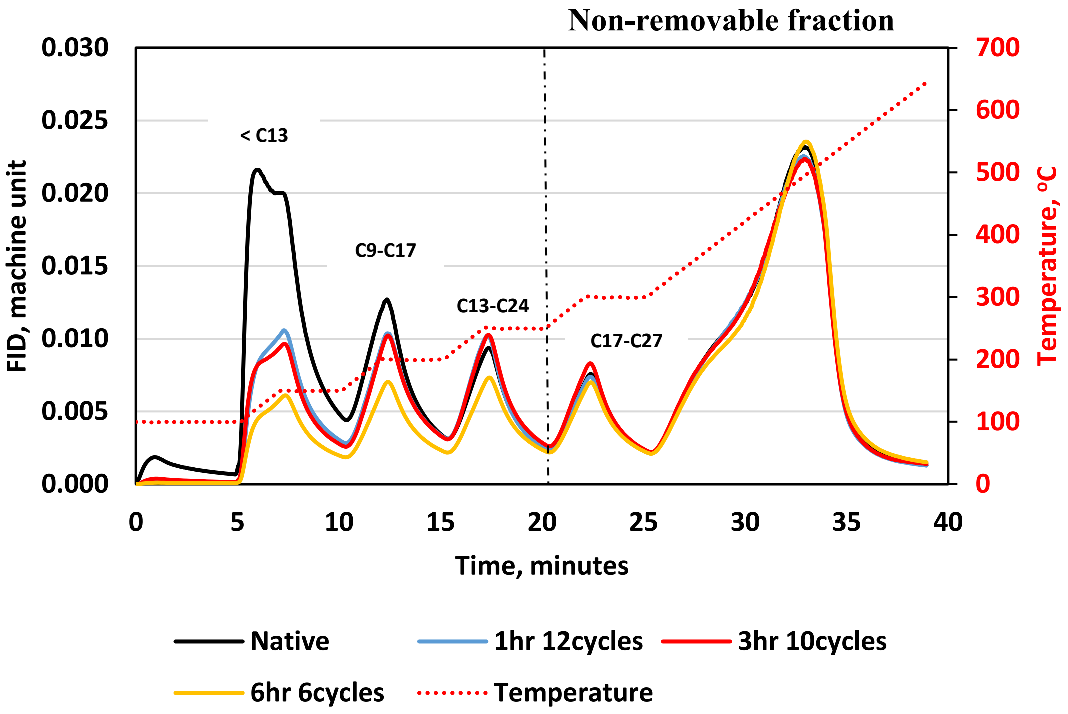

Figure 38: HAWK pyrograms for different soaking time experiments. Modified HAWK protocol allows the finer resolution of the S1 signal to four different hydrocarbon fractions. Note that right side of the vertical dotted line represent the non-removable fraction.

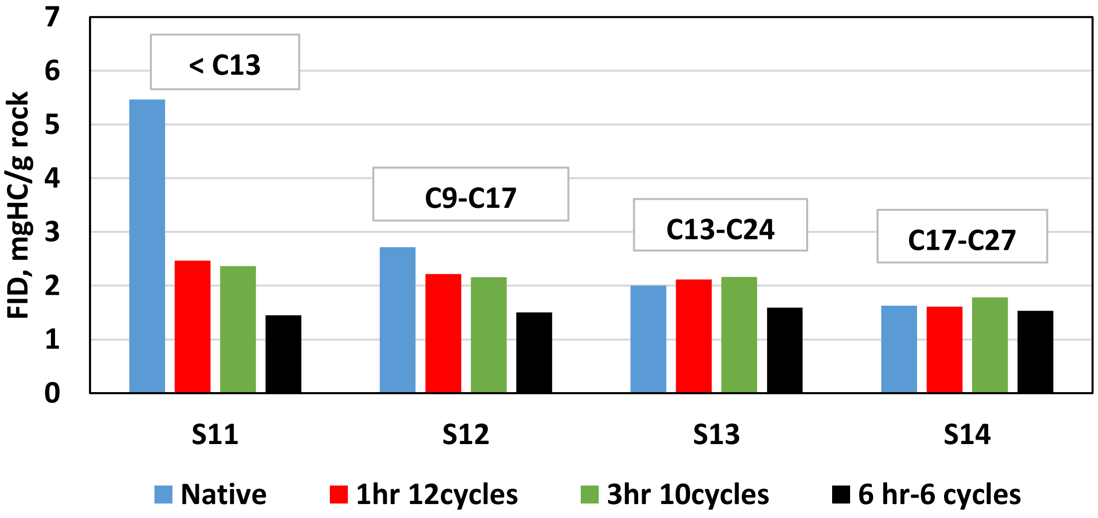

Figure 39: Summary of HAWK analyses regarding effect of soaking time. Each signal represents residual hydrocarbons inside of rock. Therefore, lower FID signal from huff-n-

puff tests represents more recovery of HCs. Note that six hour soak had 20% reduction in S13 peaks (heavier hydrocarbons).

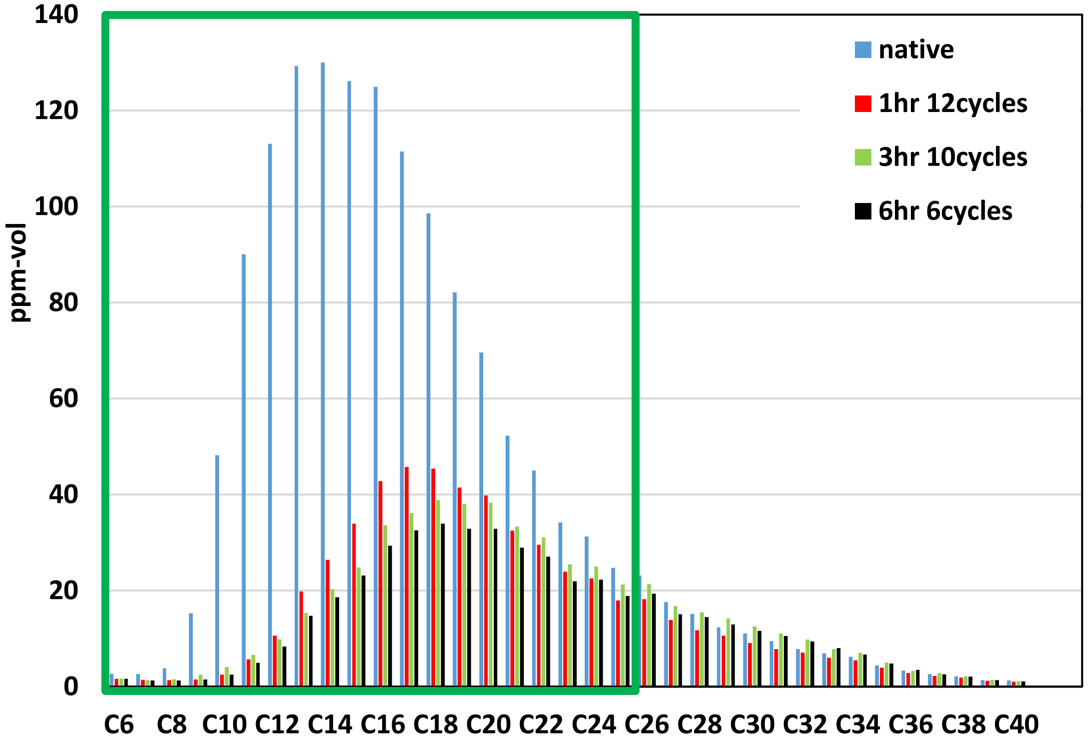

Figure 40: GC chromatograms of residual fluids as a function of soaking time. Most hydrocarbon production is the result of mobilizing HC molecules < C25.

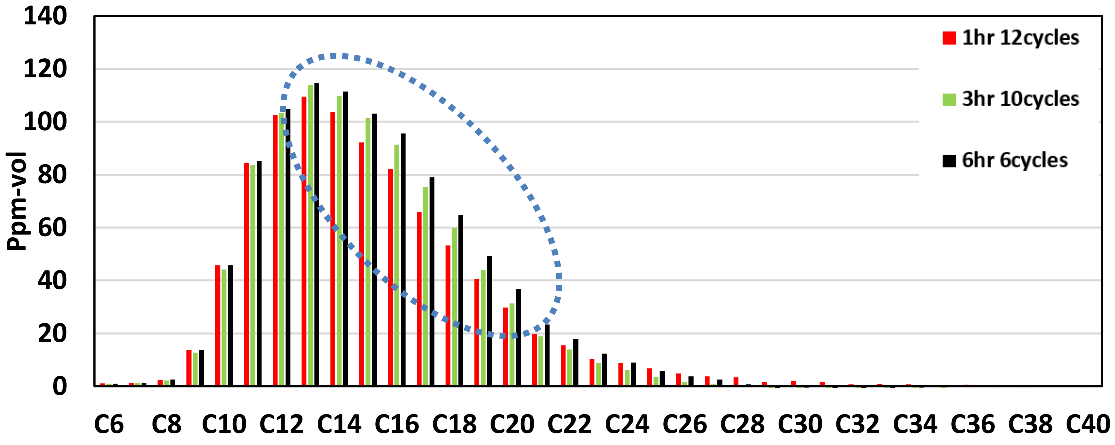

Figure 41: Difference plot of GC chromatograms of residual rock with respect to soaking time. This plot indicates the produced hydrocarbon. Note that longer soaking time can produce slightly heavier hydrocarbons.

4.3 Impacts of injection pressure and injection rate for Huff-n-puff EOR

Table 6 shows the matrix of experiment studied.

Table 6: Matrix of experiments for investigating injection pressure and rate effects. Sample sizes were 7-8mm and the amount of sample used in each experiment was about 22 grams. Production time for all the tests were one hour.

Crushed sample tests				
Test #	**Soak Time(hr)**	**# Cycle**	**Gas**	**Pressure(psi)**
4	1	3	Mixed gas C1:C2 (72:28)	2500
5	1	6	Mixed gas C1:C2 (72:28)	3500
6	1	6	Mixed gas C1:C2 (72:28)	4500
7	1	12	Field gas*	2000
8	1	5	Field gas*	4000
9	1	10	Mixed gas C1:C2 (72:28)	5500
10	1	3	Mixed gas C1:C2 (72:28)	4500,5500,6500
11	0	6	Mixed gas C1:C2 (72:28)	4500

*C1:C2:C3-C8 (76:13:11)

4.3.1 Injection pressure above/below MMP

Figs. 42 through **44** show the T_2 distributions for the Eagle Ford samples after each huff-n-puff cycle for 1000 psi below MMP, at MMP, and 1000 psi above MMP, which corresponds to test 4, test 5 and test 6, respectively. When injection pressure is 1000 psi below MMP, T_2 amplitude reduction is not very significant (**Fig. 42)**. However, at an injection pressure at MMP and 1000 psi above MMP behavior of T_2 spectra are very similar in that both have a significant reduction in T_2 amplitude in T_2 region of 1ms to 30ms (see **Fig. 43** and **Fig. 44)**. The recoveries after 3rd cycle are 8%, 22%, and 25% for 1000 psi below MMP, at MMP, and 1000 psi above MMP, respectively (**Fig. 45**). It is worth noting that recovery at MMP and 1000 psi above MMP did not exhibit a significant difference. Further investigation and discussion will be made in the next subsection.

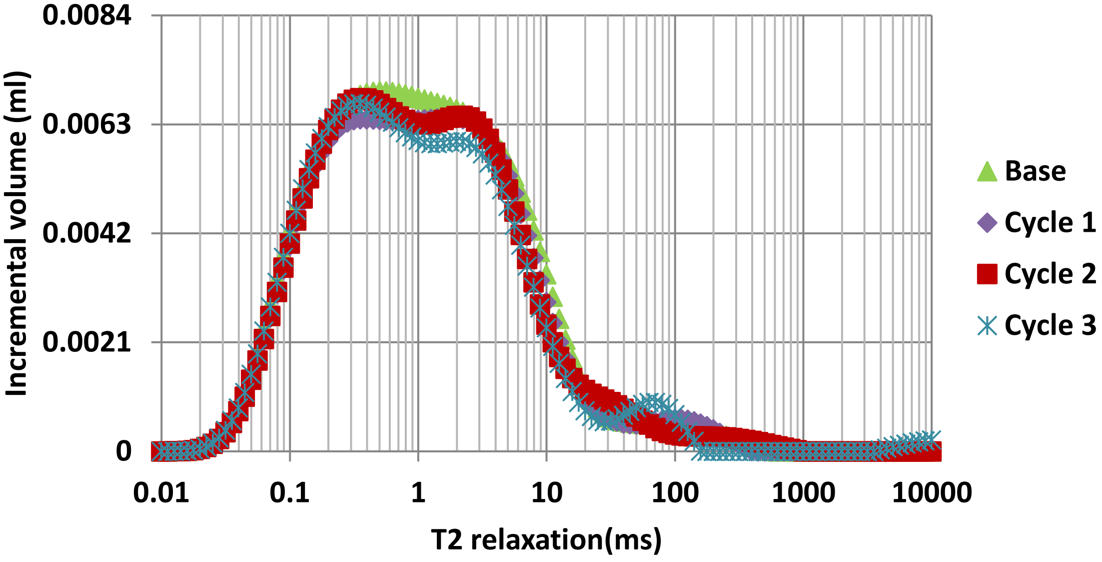

Figure 42: Successive T_2 spectra of test 4 (3 cycles with one hour soaking time. Mixed gas C1:C2 (72:28) was injected at 2500 psi, which is 1000 psi below MMP). Note that T_2 amplitude reduction during huff-n-puff cycles is insignificant under immiscible conditions.

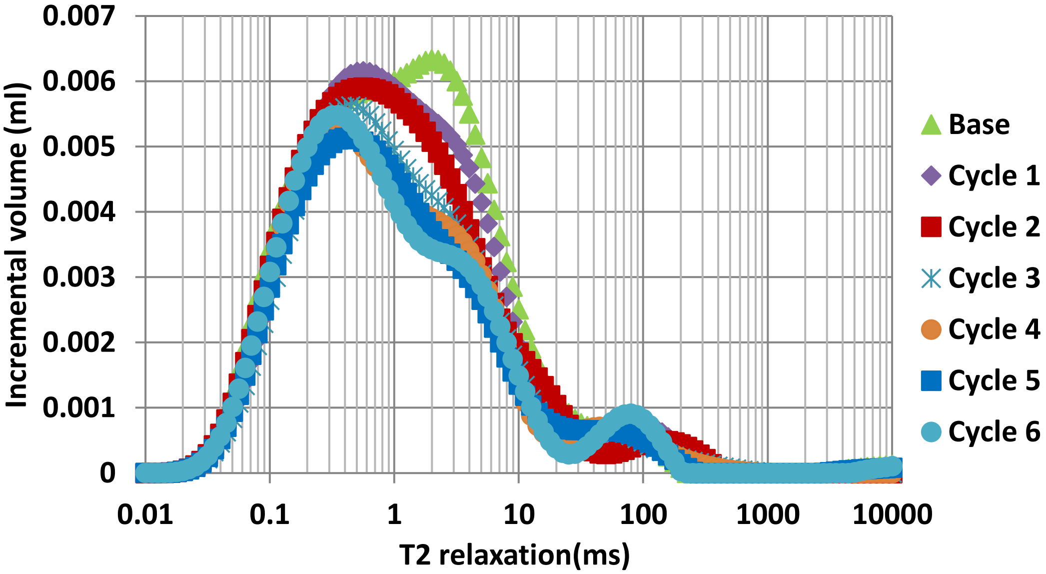

Figure 43: Successive T_2 spectra of test 5 (6 cycles with one hour soaking time. Mixed gas C1:C2 (72:28) was injected at 3500 psi, which is at MMP). Note that NMR volumes between T_2 relaxation regions of 1ms to 30ms are preferentially decreasing. This indicates that light hydrocarbon or fluid in larger pores is produced during the huff-n-puff.

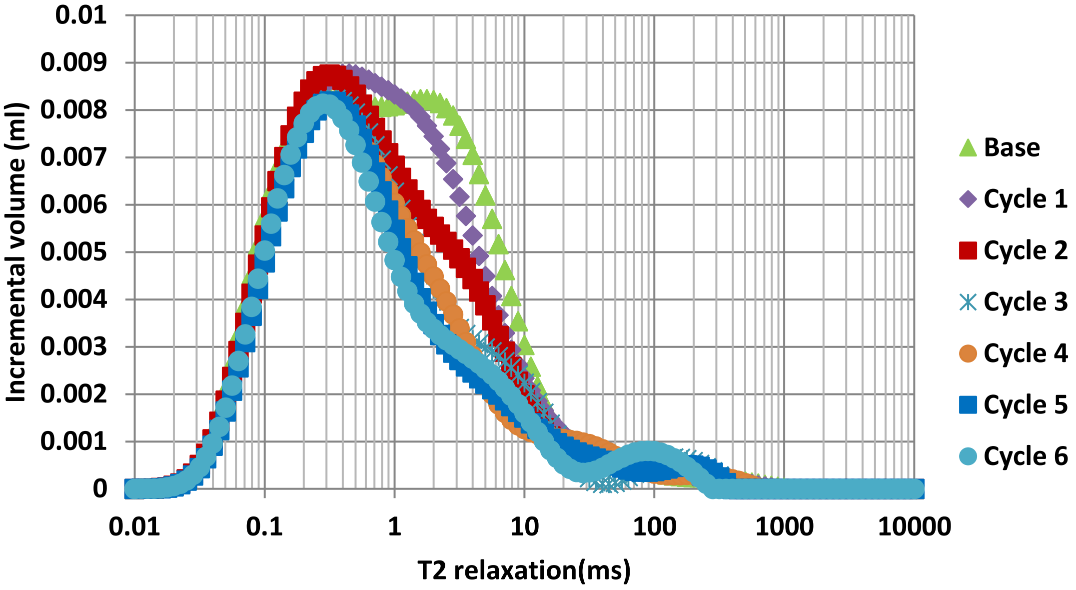

Figure 44: Successive T_2 spectra of test 6 (6 cycles with one hour soaking time. Mixed gas C1:C2 (72:28) was injected at 4500 psi, which is 1000 psi above MMP). Note that NMR volumes between T_2 relaxation regions of 1ms to 30ms are preferentially decreasing. This indicates that light hydrocarbon or fluid in the larger pores is produced during the huff-n-puff.

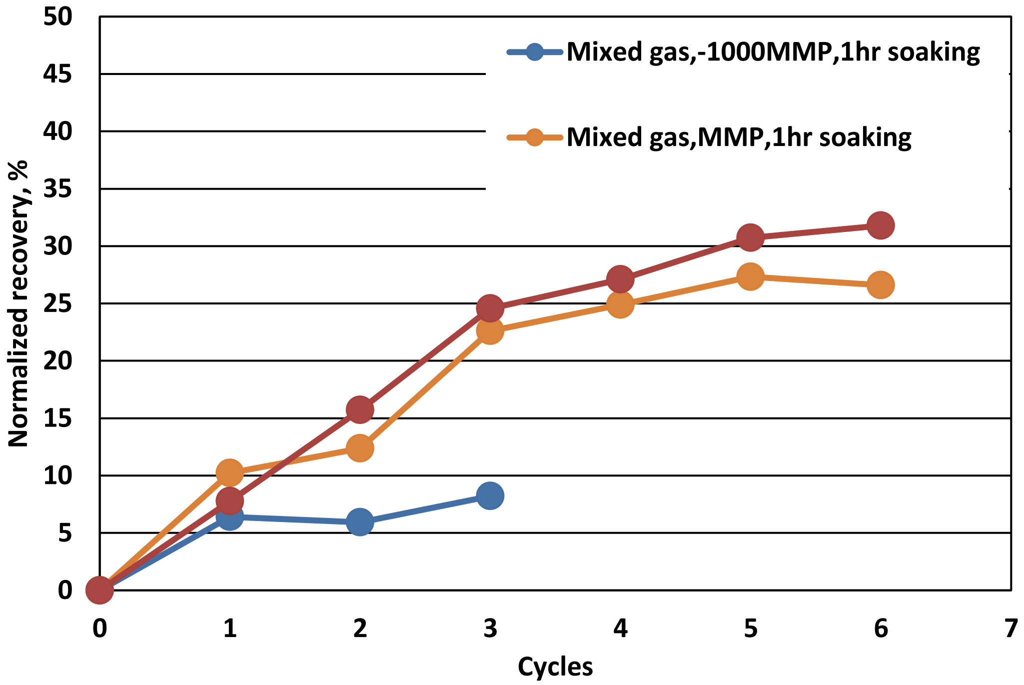

Figure 45: Summary of recovery versus cycles from three different injection pressures using mixed gas C1:C2 (72:28). Recovery at the 3rd cycle of each experiments is 25%, 22%, and 8% in 1000 psi above MMP, at MMP, and 1000 psi below MMP, respectively. Each cycle has 2 hr of residence time.

A similar study was conducted using field gas. **Fig. 46** and **Fig. 47** show the T_2 spectra after each huff-n-puff cycle for 1000 psi below MMP and 1000 psi above MMP, which corresponds to test 7 and test 8, respectively. Results are very similar to the study conducted with C1:C2 (72:28) mixed gas. When injection pressure was below MMP by 1000 psi, recovery is significantly lower compared to when the injection pressure was above MMP by 1000 psi (**Fig. 48**). GC analysis on residual fluids after 12 cycles of huff-n-puff at 1000 psi below MMP is shown in **Fig. 49**. This showed that the hydrocarbon fraction only up to C19 was produced. When injection pressure was 1000 psi above MMP, hydrocarbon fraction produced was up to C25 (see **Fig. 40**). This indicates that injection pressure affects the fraction of hydrocarbons produced during the huff-n-puff EOR. Even though GC results from 1000 psi above MMP is from mixed gas C1:C2(72:28) and GC result from 1000 psi below MMP are from field gas, recall that composition of field gas (**Table 6**) and mixed gas C1:C2(72:28) are quite similar allowing the comparison of GC results regarding injection pressure. Further evidence that mixed gas C1:C2 (72:28) can be used as proxy gas for field gas will be discussed in the later section.

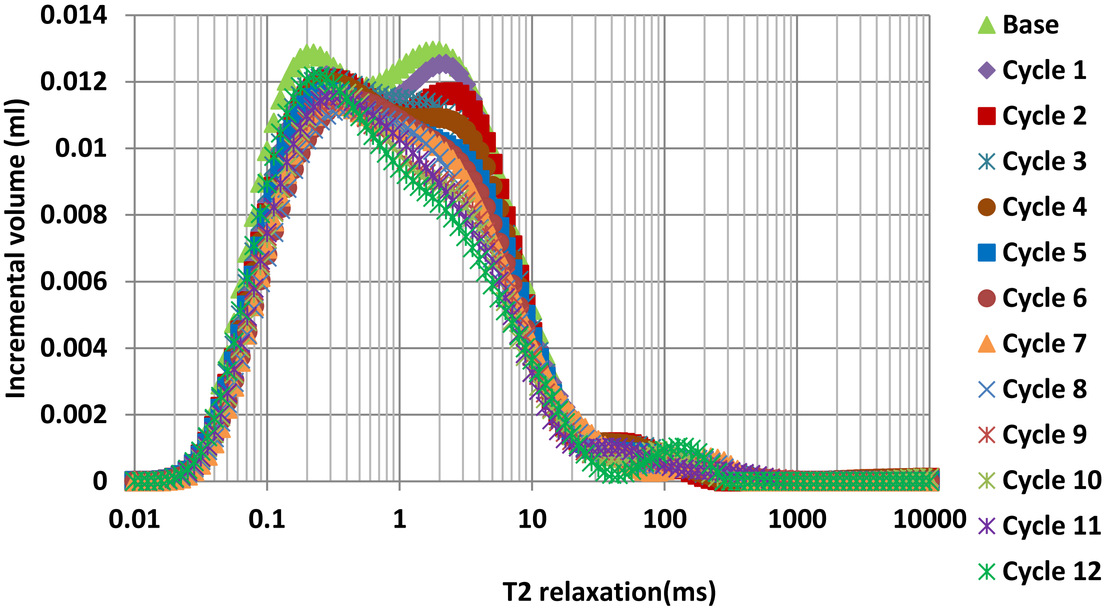

Figure 46: Successive T_2 spectra of test 7 (12 cycles with one hour soaking time. Field gas was injected at 2000 psi, which is 1000 psi below MMP). Note that NMR volumes between T_2 relaxation regions of 1ms to 30ms are preferentially decreasing. This indicates that light hydrocarbon or fluid in larger pores is produced during the huff-n-puff.

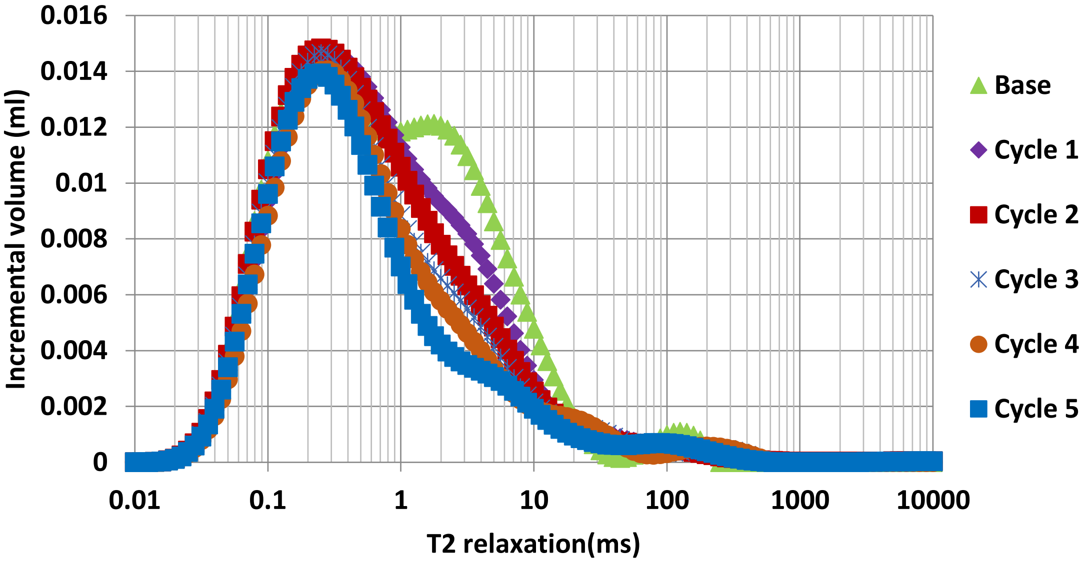

Figure 47: Successive T_2 spectra of test 8 (5 cycles with one hour soaking time. Field gas was injected at 4000 psi, which is 1000 psi above MMP). Note that NMR volumes between T_2 relaxation regions of 1ms to 30ms are preferentially decreasing. This indicates that light hydrocarbon or fluid in larger pores is produced during the Huff-n-puff.

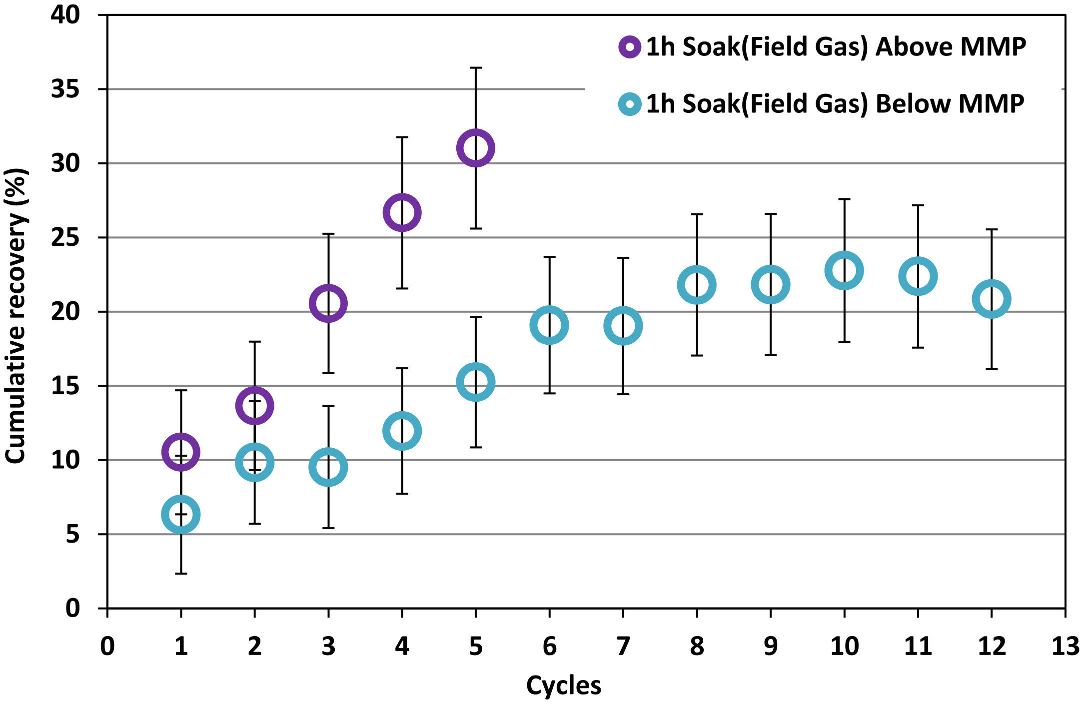

Figure 48: **Summary of recovery versus cycles from two different injection pressures using field gas. Recoveries at the 5th cycle of each experiments are 31% and 15% in 1000 psi above MMP and 1000 psi below MMP, respectively, a factor of 2 difference. Each cycle has 2 hr of residence time.**

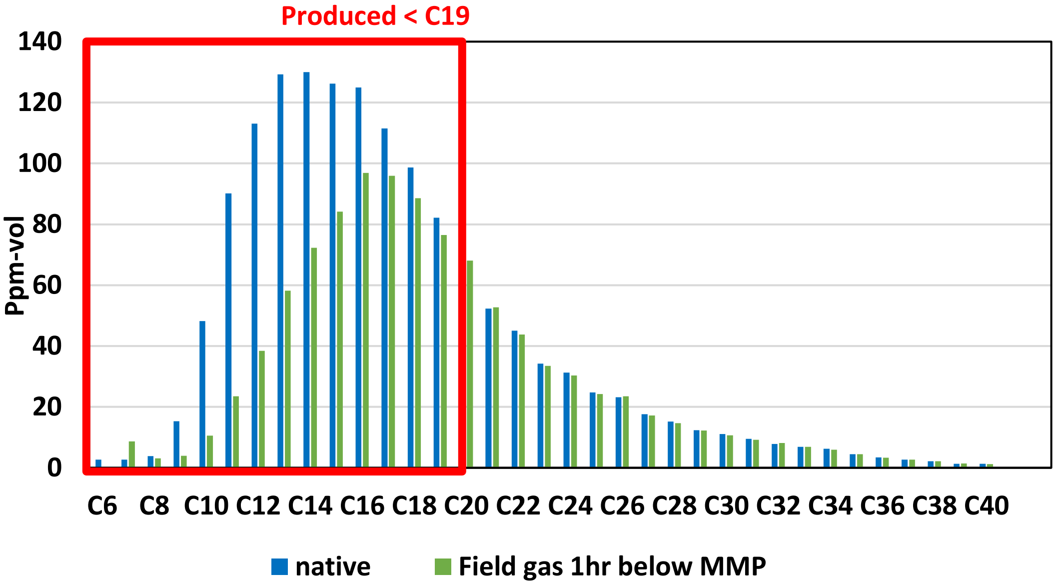

Figure 49: **GC chromatogram analysis on residual fluids after huff-n-puff EOR using field gas at 1000 psi below MMP. Hydrocarbons are only produced up to C19.**

4.3.2 Injection pressure above MMP

In previous section, it was shown that the recovery from injection pressure at MMP and at 1000 psi above MMP were similar. To further investigate the effect of injection pressure, two experiments were conducted; first, **Fig. 50** is the T_2 distributions for the remaining fluid in the Eagle Ford samples after each huff-n-puff cycle for 2000 psi above MMP (test 9). Comparison recovery plot between 2000 psi above MMP case and 1000 psi above MMP indicates that recovery is very similar regardless of the higher injection pressure (**Fig. 51)**. Second, **Fig. 52** is the T_2 distributions for the remaining fluid in the Eagle Ford sample after each huff-n-puff cycle for varying injection pressure above MMP, which corresponds to test 10. For example, during first cycle, injection pressure was 4500 psi (1000 psi above MMP). During second cycle, injection pressure was 5500 psi (2000 psi above MMP). Finally, during third cycle, injection pressure was 6500 psi (3000 psi above MMP). T_2 amplitude reduction is observed mostly in 1-30ms region again, which seems to be consistent with all other experiments. **Fig. 53** shows the recovery comparison between the 1000 psi above MMP case and varying injection pressure case. The results suggest that recoveries were very similar regardless of excess pressure for injection per each cycle. Both experiments suggest that extra injection pressure above MMP does not yield additional recovery. There can be two possible explanations for this phenomenon; first, the sample are 7-8mm size crushed samples. This size is sufficiently small that one hour soaking time is sufficient for injection gas to permeate throughout the whole sample. In another words, pressure gradient from the outer surface of sample and inside of sample can reach equilibrium in one hour with 7-8mm size. If the sample size becomes larger as at the core scale, extra injection pressure may contribute to additional recovery. Second, the diffusion coefficient generally increases with the pressure; however, it started to decrease above MMP (**Fig. 54**). This can ultimately reduce the rate of injection gas.

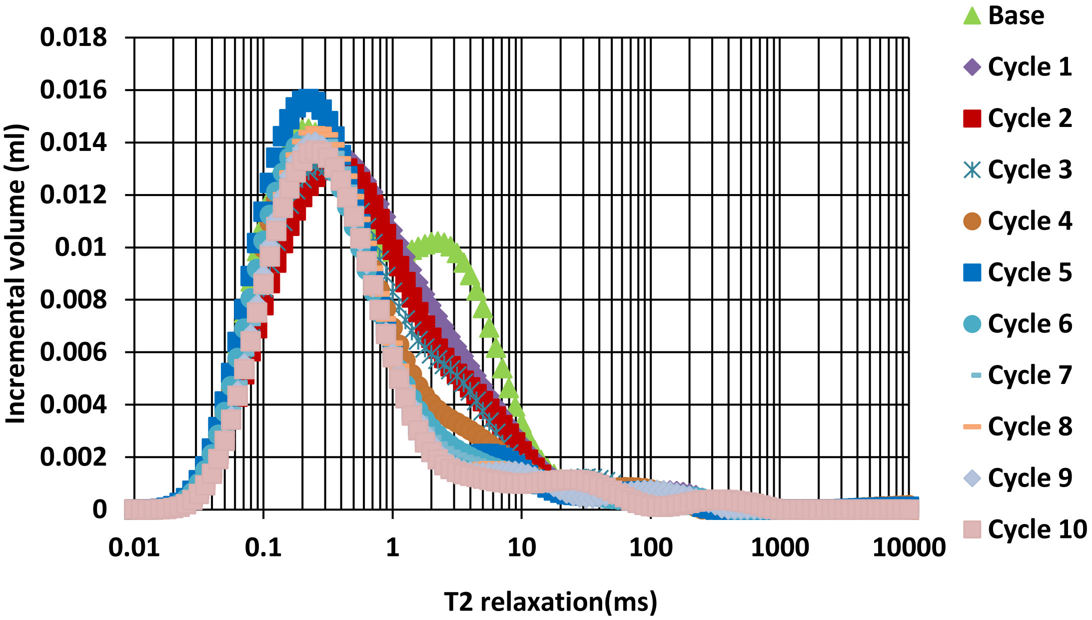

Figure 50: Successive T_2 spectra of test 10 (10 cycles with one hour soaking time. Mixed gas C1:C2 (72:28) was injected at 5500 psi, which is 2000 psi above MMP). Note that NMR volumes between T_2 relaxation regions of 1ms to 30ms are preferentially decreasing. This indicates that light hydrocarbon or fluid in larger pores is produced during the Huff-n-puff.

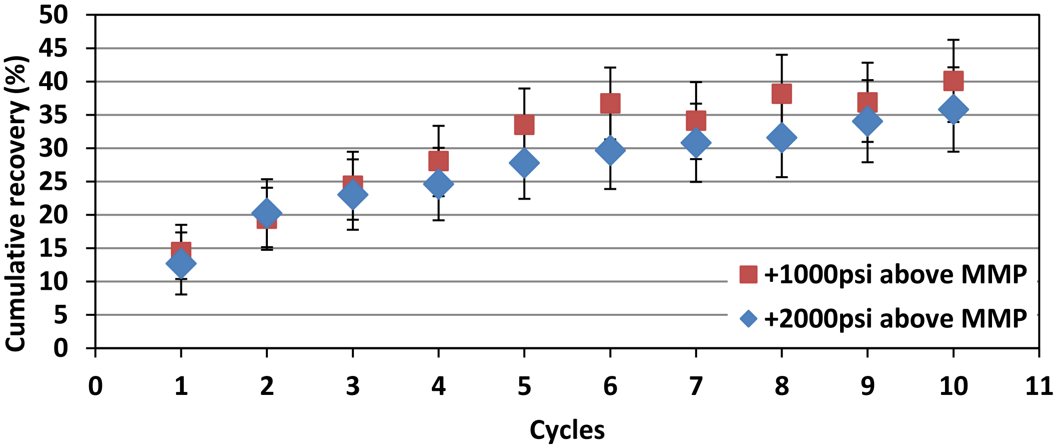

Figure 51: Summary of recovery versus cycles from two different injection pressures. Recoveries at the end of each experiments are 40% and 36% in 1000 psi above MMP and 2000 psi above MMP, respectively. Each cycle has 2 hr of residence time.

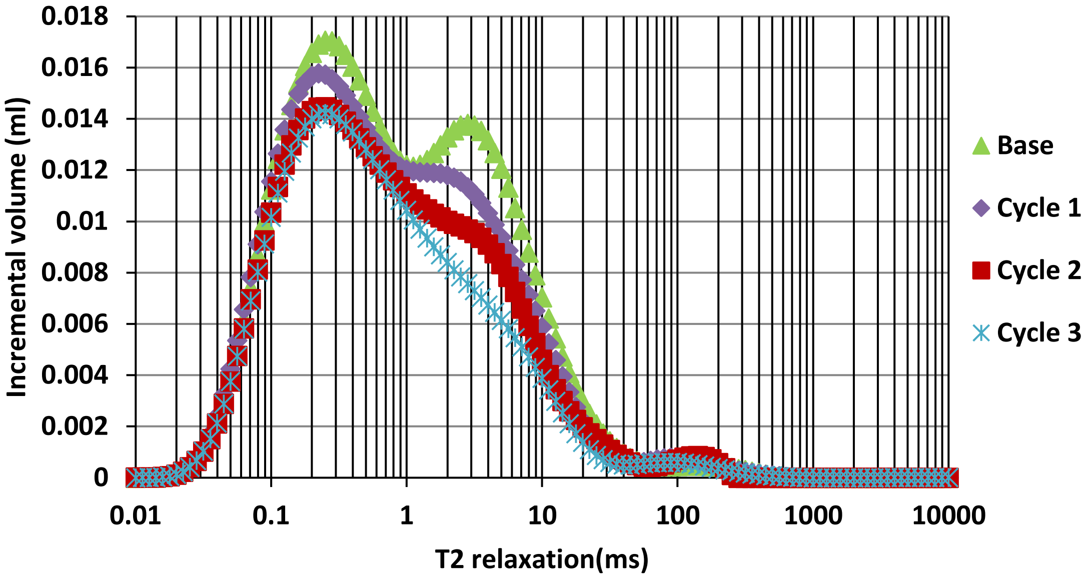

Figure 52: Successive T_2 spectra of test 10 (3 cycles with one hour soaking time. Mixed gas C1:C2 (72:28) was injected at 4500 psi (1000 psi above MMP) for cycle 1, 5500 psi (2000 psi above MMP) cycle 2, and 6500 psi for cycle 3 (3000 psi above MMP)). Note that NMR volumes between T_2 relaxation regions of 1ms to 30ms are preferentially decreasing. This indicates that light hydrocarbon or fluid in larger pores is produced during the Huff-n-puff.

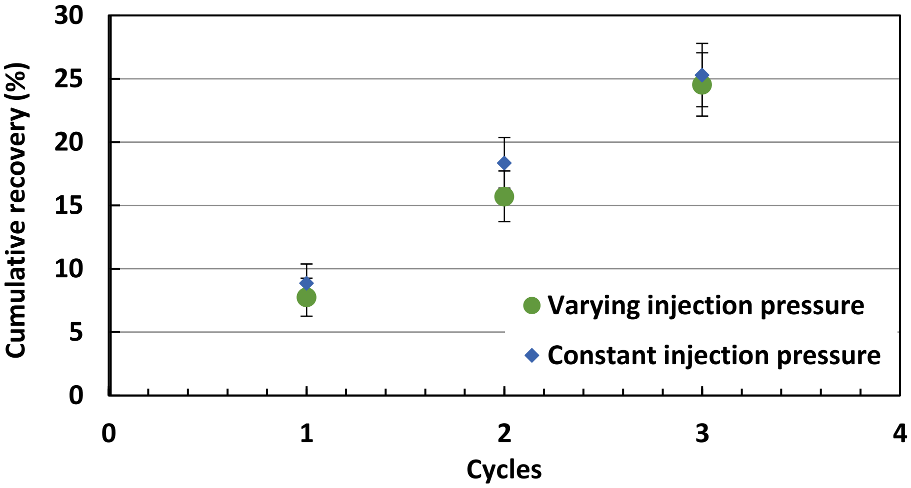

Figure 53: Comparison of recovery as a function of injection pressure above MMP using mixed gas C1:C2 (72:28). Green symbol represents constant injection pressure of 1000 psi above MMP. Blue symbol represents injection pressure varying from 1000 psi above MMP (cycle 1), 2000 psi above MMP (cycle 2), and 3000 psi above MMP (cycle 3). Recoveries at the end of each experiment are 24.5% and 25.2% in constant injection pressure and varying injection pressure experiments, respectively. Each cycle has 2 hr of residence time.

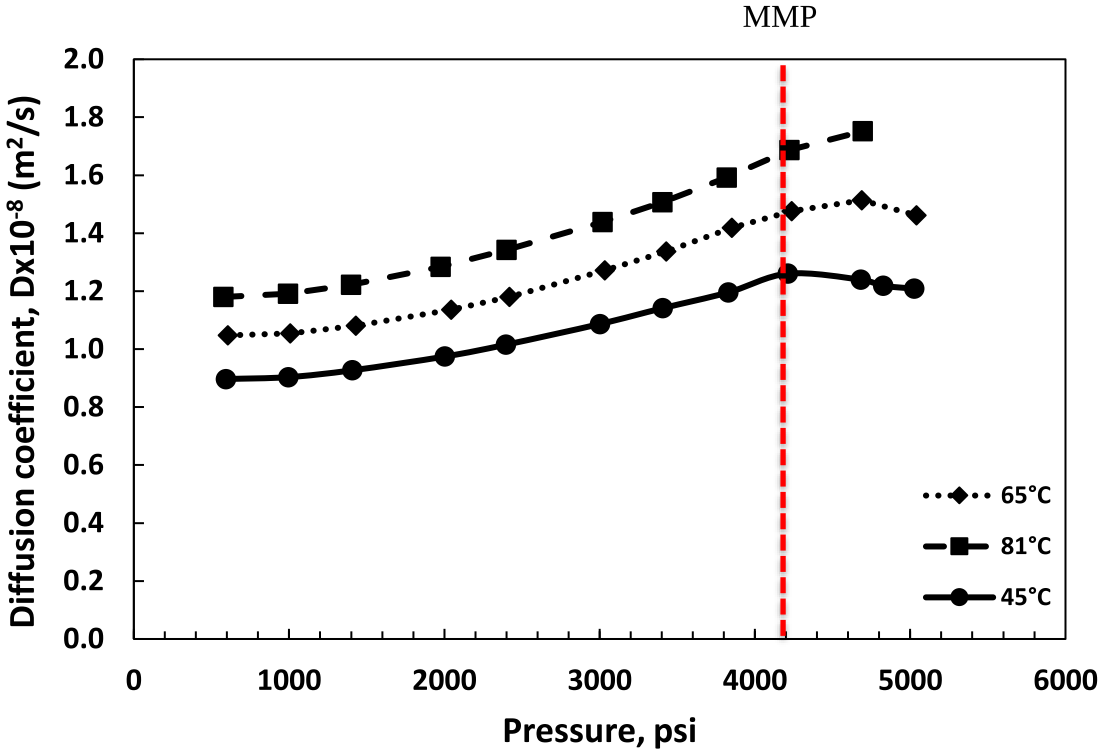

Figure 54: Diffusion coefficient of methane in dodecane as a function of pressure for different temperatures. Digitized and modified from Jamialahamadi et al., 2006.

4.3.3 Injection gas rate

Recovery from huff-n-puff experiments with two different injection rates were compared: high injection rate of 30 cc/min and low injection rate of 1.5 cc/min. For a soaking time of 1 hour, the MMP was achieved in few minutes with high injection rate. Whereas, it took a longer time (40 minutes) to achieve MMP with low injection rate. All the tests in this study used the high injection rate of 30 cc/min except for test 11. **Fig. 55** shows T_2 spectra of test 11. Reduction in T_2 amplitude is not significant except for the first cycle. Recovery comparison is made between low injection rate and high injection rate (**Fig. 56**). Recovery up to three cycles appears to be very similar. However, after third cycle, recovery in low injection rate started to plateau where high injection rate recovery kept increasing. For a fixed soaking time (1 hour in this experiment), low injection rate results in sample being below MMP for a much longer duration as compared to when using high injection rate. As shown earlier, recovery is always low when the injection pressure is below MMP. This explains the results seen in **Figure 56**.

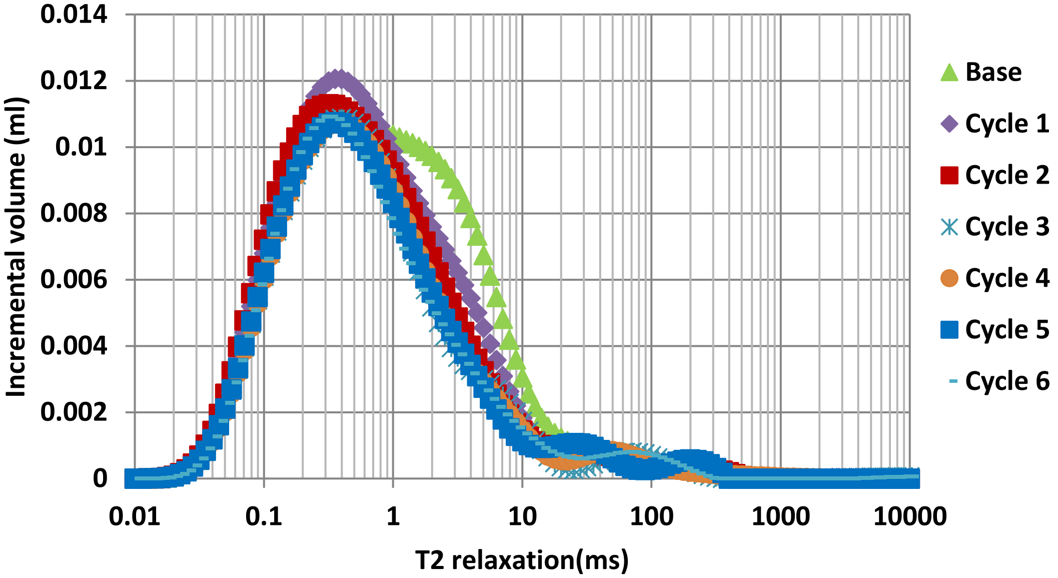

Figure 55: Successive T_2 spectra of test 11. 6 cycles with low injection rate. Mixed gas C1:C2 (72:28) was injected at 4500 psi (1000 psi above MMP). Note that NMR volumes between T_2 relaxation regions of 1ms to 30ms are preferentially decreasing. This indicates that light hydrocarbon or fluid in larger pores is produced during the huff-n-puff.

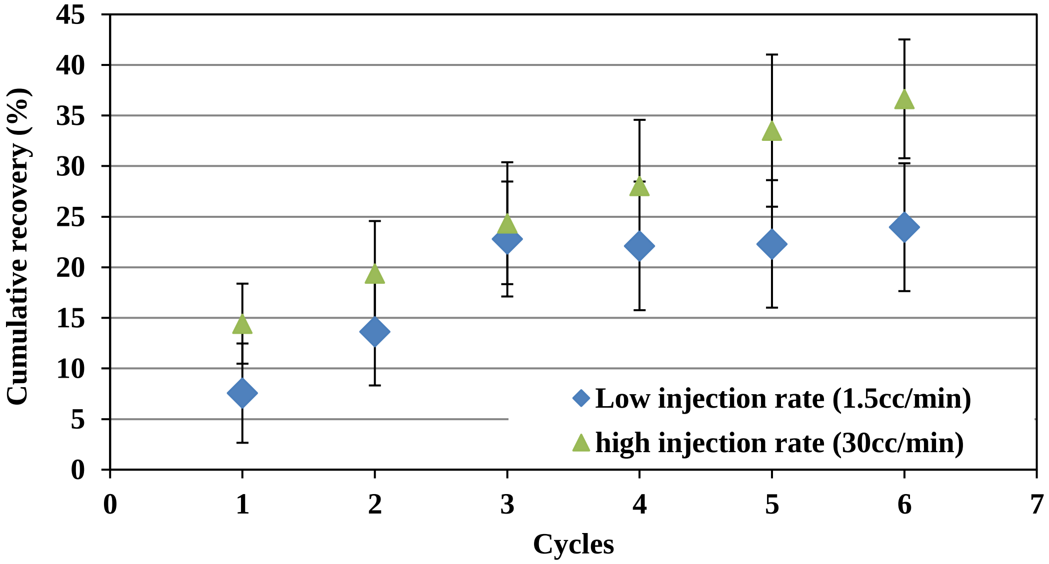

Figure 56: Comparison of recovery versus cycles from two different injection rates. Recoveries at the end of each experiment are 37% and 24% in high injection rate and low injection rate, respectively. Lower recovery for low injection rate is attributed to sample being at below MMP for most of the time during soaking period. Each cycle has 2 hr of residence time.

4.4 Impact of gas composition on recovery

Table 7 shows the matrix of experiment to evaluate injectate composition on EOR recovery.

Table 7: Matrix of experiments for investigating impact of different injection gases. Preserved sample sizes were 7-8mm and the amount of sample used for each experiment was about 22 gm. Production time for all the tests was one hour.

Crushed sample tests				
Test #	Soak Time(hr)	# Cycle	Gas	Pressure above MMP (psi)
12	1	5	CO_2	+1000 (MMP=2500 psi)
13	1	4	C2	+3000 (MMP=1000 psi
14	1	10	Mixed gas C1:C2 (95:5)	+1000 (MMP=5000 psi)

Fig. 57 and **Fig. 58** show successive T_2 spectra of CO_2 and C2; both exhibit a reduction in T_2 amplitude between T_2 regions of 0.1ms to 30ms. These T_2 reductions in T_2 region of 0.1ms to 1ms may indicates that either fluids in small pore is produced or heavy hydrocarbons are mobilized.

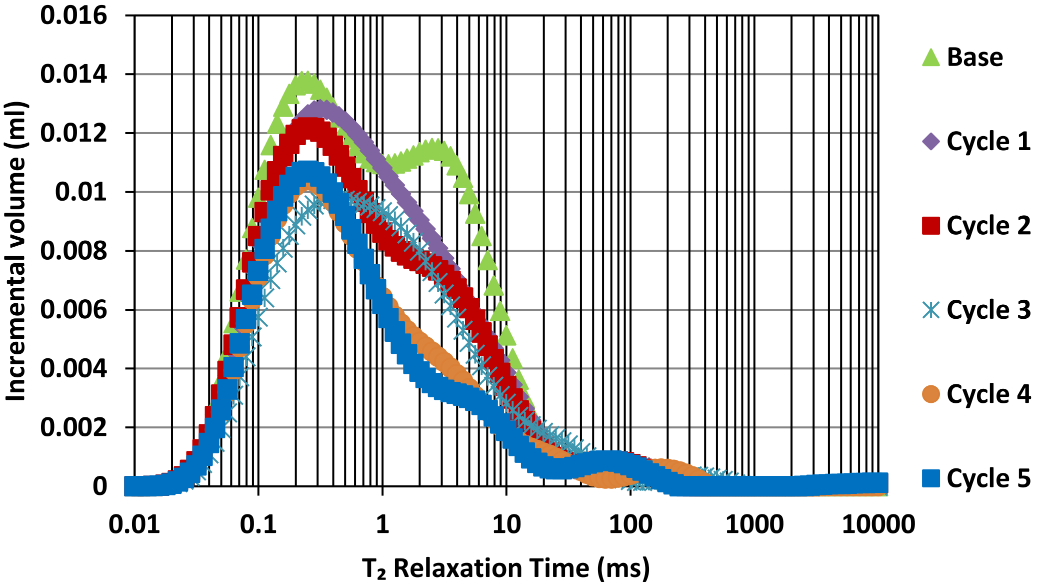

Figure 57: Successive T_2 spectra of test 12. Five cycles with one hour soaking time. CO_2 was injected at 3500 psi (1000 psi above MMP). Note that NMR volumes between T_2 relaxation region of 0.1ms to 30ms are decreasing. This indicates that not only light hydrocarbons or fluids in larger pores are produced but also heavy hydrocarbon or fluids in small pores are produced during huff-n-puff cycles.

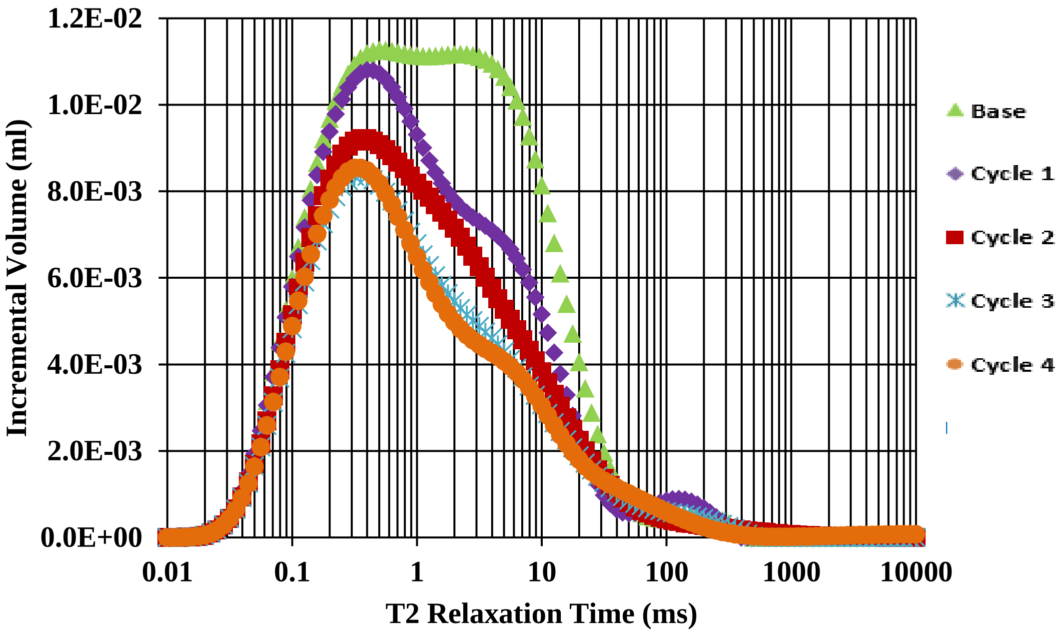

Figure 58: Successive T_2 spectra of test 13. Four cycles with one hour soaking time. C2(ethane) was injected at 4000 psi (3000 psi above MMP). Note that NMR volumes between T_2 relaxation region of 0.1ms to 30ms are decreasing. This indicates that not only light hydrocarbons or fluids in larger pores are produced but also heavy hydrocarbon or fluids in small pores are produced during huff-n-puff cycles.

In contrast to ethane and CO_2 T_2 NMR behavior for tail gas exhibits reduction in T_2 amplitude only between 1ms to 30ms (**Fig. 59**). This indicates that tail gas does not have the ability to produce fluids in small pore or heavier hydrocarbons due to high methane concentrations. However, ethane and CO_2 have ability to produce heavier hydrocarbon as shown in **Fig. 60**. Ethane has the most impact on S13 and S14 pyrolysis peaks, especially S14 peak. CO_2 has some impact on S13 peak as well. This result highlight the potential benefit of enriching gas. McGuire et al. (2017), Hawthorne and Miller (2019) have also shown richer hydrocarbon gas will be superior to leaner gas for dissolving crude oil hydrocarbon when used for EOR. Finally, **Fig. 61** shows the summary of recovery profile with different solvent gases. The performance in recovery efficiency at the same test configuration are in the following order; Ethane > CO_2 > C1:C2 (72:28) ≈ Field gas > C1:C2 (95:5)

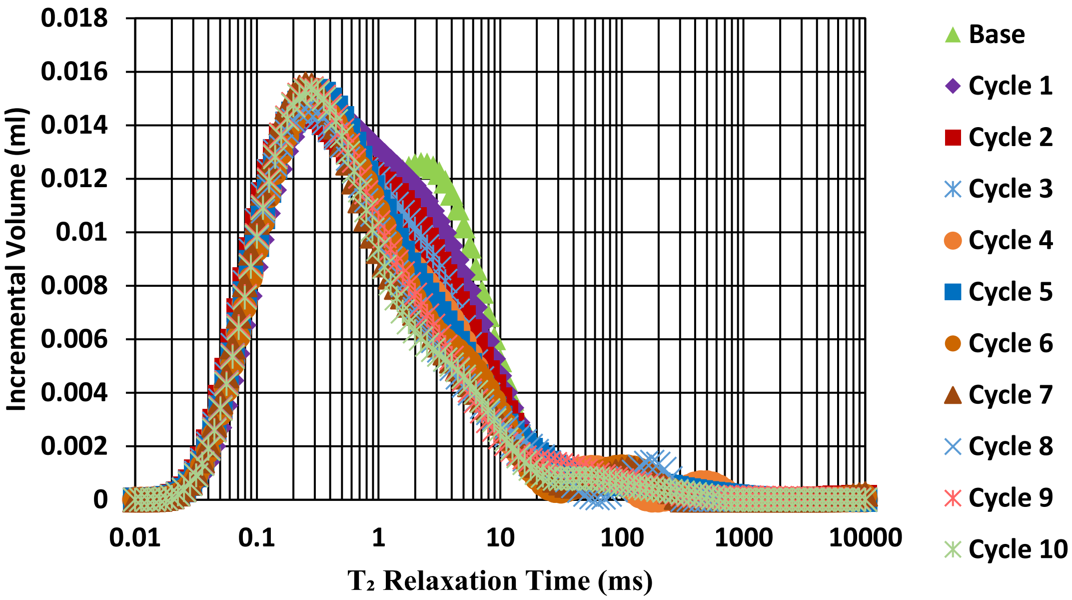

Figure 59: Successive T_2 spectra of test 14. Ten cycles with one hour soaking time. Mixed gas C1:C2 (95:5) was injected at 6000 psi (1000 psi above MMP). Note that NMR volumes between T_2 relaxation region of 1 ms to 30 ms are preferentially decreasing. This indicates that light hydrocarbons or fluid in larger pores are produced during the huff-n-puff.

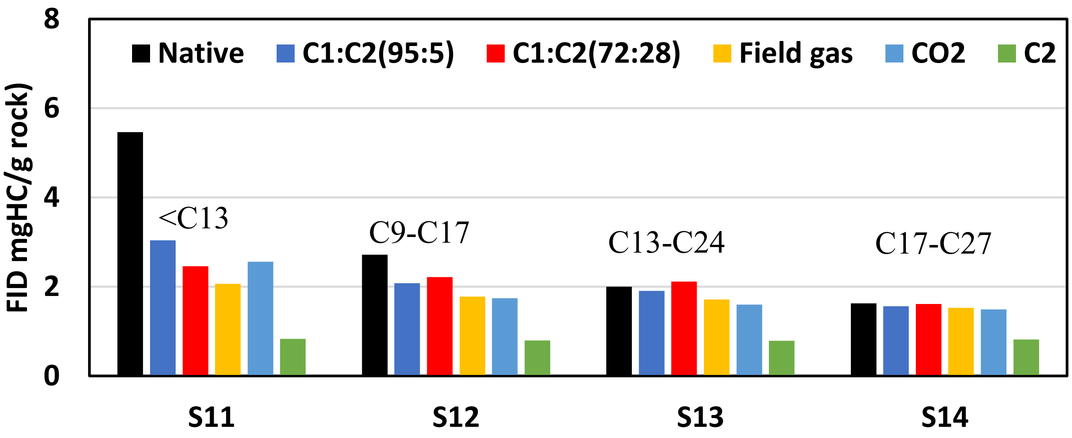

Figure 60: Summary of HAWK pyrolysis results with regards to the effect of different solvent gases. Results suggested that ethane (C2) is the most efficient solvent gas where other solvent does not have a major impact on S13 and S14 pyrolysis peaks (heavier hydrocarbons). Note that ethane had 65% and 50% reduction in S13 and S14 pyrolysis peaks respectively.

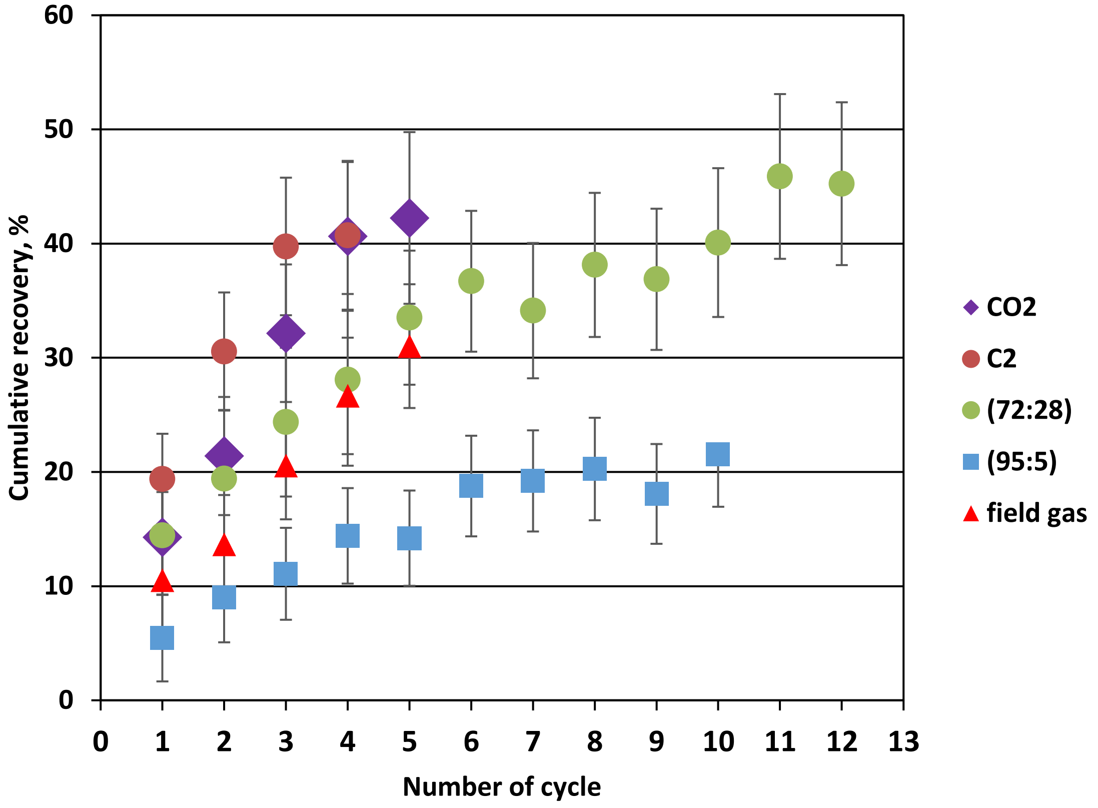

Figure 61: Summary of recovery versus cycles for different types of solvent gas. Ethane has the highest recovery followed by CO_2. Mixed gas C1:C2(72:28) perform similar as field gas, which indicates that mixed gas C1:C2(72:28) can used as proxy gas for a field gas. Tail gas (C1:C2(95:5)) performed the worst due to its high methane concentration. Note that all these test configurations are 7-8 mm size, preserved sample state, one hour soaking, and one hour production. Each cycle has 2 hr of residence time.

4.5 Impact of surface area on recovery

Impact of surface area was investigated by using crushed sample size of 0.9-2 mm to compare with 7-8 mm size. **Table 8** shows the matrix of experiment studied.

Table 8 Matrix of experiments for investigating surface area. Sample sizes were 0.9-2mm and the amount of sample used for each experiment was about 22 grams. Production time for all tests was one hour.

Crushed sample tests (0.9-2 mm)				
Test #	**Soak Time(hr)**	**# Cycle**	**Gas**	**Pressure(psi)**
15	1	5	CO_2	3500
16	1	5	C2	4000

Fig. 62 shows the successive T2 spectra for test 15 (CO_2). Notice that first cycle has a large reduction in T2 amplitude. **Fig. 63** shows the recovery comparison between two sample sizes; 0.9-2mm and 7-8mm. 0.9-2 mm crushed sample (BET surface area= 1.2 m^2/g) has higher recovery than 7-8 mm crushed sample (BET surface area= 0.8 m^2/g) by factor of 1.5. This is most likely due to greater surface area in smaller size sample. Test with ethane also showed very similar results as shown in **Fig. 64** and **Fig. 65**. These tests highlight the importance of surface area and the need to understand the details of the stimulated reservoir volume. Completion strategy and design become among the most important factors regarding increasing surface area. Therefore, if wells are already completed, the ones with an optimal completion design should be considered as good candidate for huff-n-puff. If wells have not been completed, completion strategy should be considered to maximize both early time production and huff-n-puff operations.

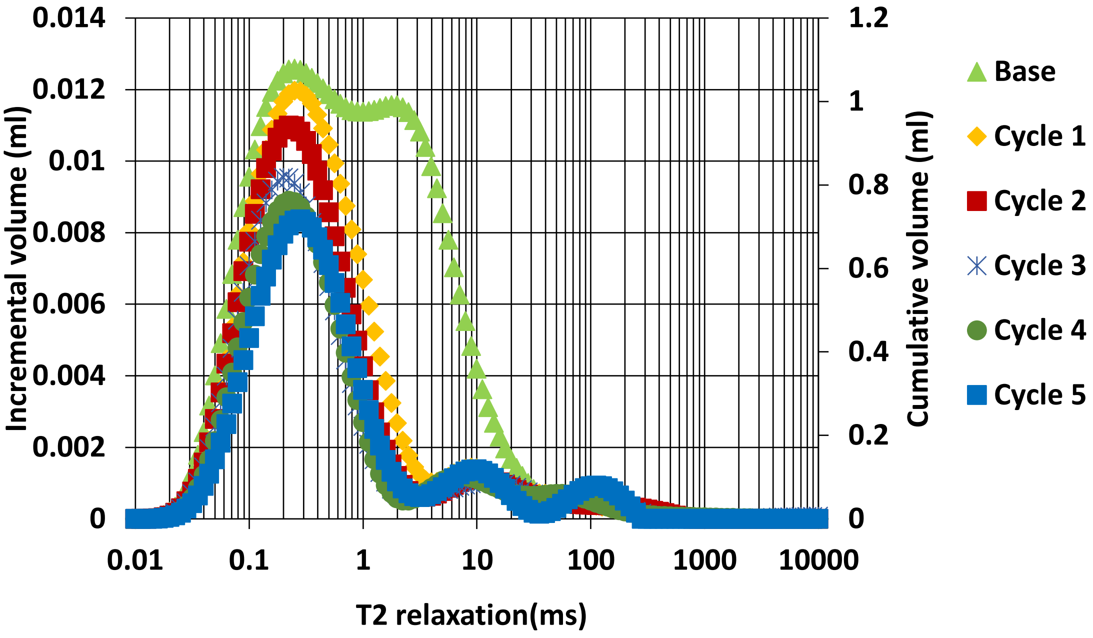

Figure 62: Successive T2 spectra of test 15. Five cycles with one hour soaking time. CO_2 was injected at 3500 psi (1000 psi above MMP). Sample size was 0.9-2mm. Note that NMR volumes between T2 relaxation region of 0.1ms to 30ms are decreasing. This indicates that not only light hydrocarbons or fluids in larger pores are selectively produced but also heavy hydrocarbons or fluids in small pores are produced during huff-n-puff cycles

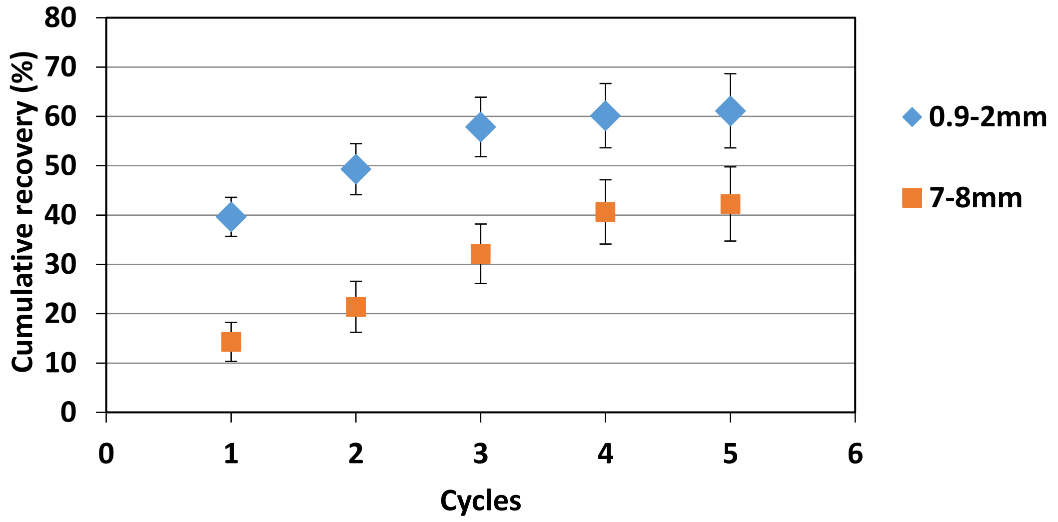

Figure 63: Comparison of recovery between two different sample sizes (CO_2). Smaller size samples (0.9-2mm) has a recovery of 61% while recovery in larger sample (7-8 mm) is 42%. 0.9-2mm size sample (BET surface area= 1.2 m^2/g) has the 1.5 times higher internal surface area than 7-8mm size sample (BET surface area= 0.8 m^2/g). Each cycle has 2 hr of residence time.

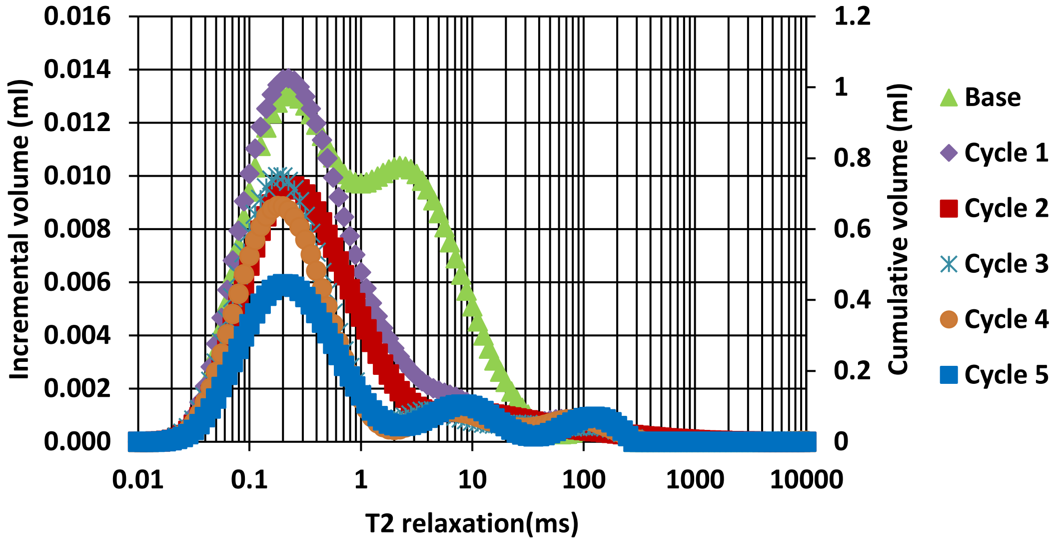

Figure 64: Successive T2 spectra of test 16. Five cycles with one hour soaking time. Ethane was injected at 4000 psi (3000 psi above MMP). Sample size was 0.9-2mm. Note that NMR volumes between T2 relaxation region of 0.1ms to 30ms are decreasing. This indicates that not only light hydrocarbons or fluids in larger pores are produced but also heavy hydrocarbons or fluids in small pores are produced during huff-n-puff cycles

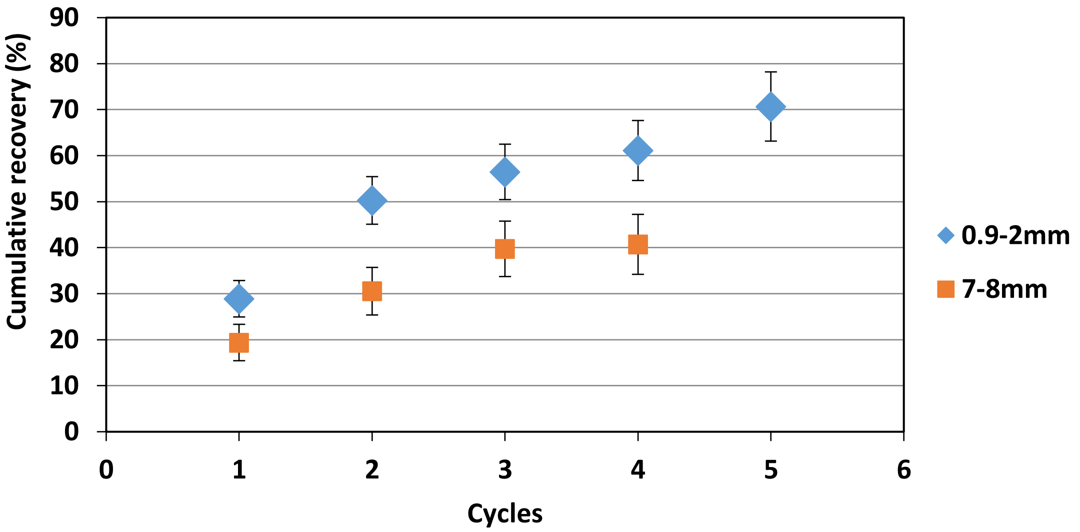

Figure 65: Comparison of recovery between two different sample sizes with ethane as the injectate. Smaller size samples (0.9-2mm) had a recovery of 61% while larger sample(7-8mm) had a yield of 40% by the 4th cycle. 0.9-2mm size sample (BET surface area= 1.2 m^2/g) has the 1.5 times higher internal surface area than 7-8mm size sample (BET surface area= 0.8 m^2/g). Each cycle has 2 hr of residence time.

Chapter 5: Conclusions

5.1 Summary

This thesis evaluates the recovery efficacy and processes in huff-n-puff gas injection experiments in preserved liquid rich shale core samples. The various key operational parameters were examined including: MMP, surface area, soaking time, injection pressure, injection gas rate and gas composition. The conclusions are summarized below for each key operation parameters.

Minimum miscibility pressure (MMP)

- Vanishing interfacial tension (VIT) technique is a fast and effective way of measuring MMP between different injectate gases and formation oils with error within ±200 psi.
- MMP value increases with increasing methane concentration in injection gas.

Soaking time

- For the sample size studied (7-8mm), residence time, i.e. the sum of soak and production times, controls the recovery rather than just the soaking time
- Longer soaking time seems to be a more economical choice in this laboratory study due to a fewer number of injection cycles needed to achieve maximum recovery. Longer soaking time also can allow operators to use the compressors on multiples wells.

Injection pressure

- Injection pressure below MMP (immiscible condition) had 17% less recovery than injection pressure above MMP (miscible condition) in field gas. Injection at or above MMP is needed to be achieved for the better recovery.
- In crushed samples (large surface area) without effective stress, excessive pressure above MMP did not yield additional recovery.
- Injection pressure determines the fraction of hydrocarbons mobilized:

1000 psi above MMP→ up to C25

1000 psi below MMP→ up to C19

Injection rate

- Higher gas injection rate (20 times higher injection rate than low injection rate) yields better recovery by factor of 1.5 than slower gas injection rate.

Injection gas composition

- The relative performance in recovery efficiency normalized to ethane for the same test configuration are:
  Ethane (100%) > CO_2 (80%) > C1:C2 (72:28) (61%) > Field gas (51%) > C1:C2 (95:5) (28%)
- Ethane is more efficient in removal of heavier hydrocarbon components than other gases. This can not only improve incremental recovery, but also improve flow conductivity in rock matrix if these components are blocking pores. This highlights the potential benefits of enriching injectate gas.

Surface area

- The sample with greater surface area (1.2 m^2/g) had 1.5 times higher recovery than the sample with less surface area (0.8 m^2/g). This highlights the importance of understanding stimulated reservoir volume (SRV) and optimal completion design for huff-n-puff gas EOR.

5.2 Future work

- Combination of huff-n-puff gas EOR with surfactant EOR can be explored in shale samples.
- The experimental work can be extended to investigate the effect of water presence in sample on recovery efficacy during the huff-n-puff gas EOR in Permian samples.
- Investigation of cracks generated during the huff-n-puff EOR, i.e. experiments with effective stress.

References

Abrams, MA., Gong, C., Garnier, C. et al. 2017. A new thermal extraction protocol to evaluate liquid rich unconventional oil in place and in-situ fluid chemistry. *Journal of Marine and Petroleum Geology* 88: 659-675. https://dx.doi.org/10.1016/j.marpetgeo.2017.09.014.

Alharthy, N., Teklu, T. W., Kazemi, H., et al. 2018. Enhanced Oil Recovery in Liquid-Rich Shale Reservoirs: Laboratory to Field. *SPE Res Eval & Eng* **21**(01): 137 - 159. SPE-175034-PA. https://doi.org/10.2118/175034-PA.

Al-Mjeni, R., Arora, S., Cherukupalli, P. et al. 2010. "Has the time come for EOR?" Oilfield Review 22.04: 16-35.

Atan, S., Ajayi, A., Honarpour, M., et al. 2018. The Viability of Gas Injection EOR in Eagle Ford Shale Reservoirs. Presented at the SPE Annual Technical Conference and Exhibition, Dallas, Texas, USA, 24-26 September. SPE-191673-MS. https://doi.org/10.2118/191673-MS.

Energy Information Administration (EIA).*Weekly U.S. Field Production of Crude Oil*,https://www.eia.gov/dnav/pet/hist/LeafHandler.ashx?n=pet&s=wcrfpus2&f=w (accessed 27 March 2019).

Gamadi, T., Sheng, J., and Soliman, M. 2013. An Experimental Study of Cyclic Gas Injection to Improve Shale Oil Recovery. Presented at the SPE Annual Technical Conference and Exhibition, New Orleans, Louisiana, USA, 30 September-2 October. SPE-166334-MS. https://doi.org/10.2118/166334-MS.

Ghedan, S. G. 2009. Global Laboratory Experience of CO2-EOR Flooding. Presented at the SPE/EAGE Reservoir Characterization and Simulation Conference, Abu Dhabi, UAE, 19-21 October. SPE-125581-MS. https://doi.org/10.2118/125581-MS.

Gupta, I. 2017. *Rock Typing in Organic Shales: Eagle Ford, Woodford, Barnett and Wolfcamp Formations*. MS thesis. University of Oklahoma, Norman, Oklahoma.

Hawthorne, S. B., Gorecki, C. D., Sorensen, J. A., et al. 2013. Hydrocarbon Mobilization Mechanisms from Upper, Middle, and Lower Bakken Reservoir Rocks Exposed to CO. Presented at the SPE Unconventional Resources Conference Canada, Calgary, Alberta, Canada, 5-7 November. SPE-167200-MS. https://doi.org/10.2118/167200-MS.

Hawthorne, S. and Miller, D. 2019. A comparison of crude oil hydrocarbon mobilization by vaporization gas drive into methane, ethane, and carbon dioxide at 15.6 MPa and 42 °C. *Fuel*. **249**: 392-399. http://dx.doi.org/10.1016/j.fuel.2019.03.118.

Hoffman, B. T., and Evans, J. G. 2016. Improved Oil Recovery IOR Pilot Projects in the Bakken Formation. Presented at the SPE Low Perm Symposium, Denver, Colorado, USA, 5-6 May. SPE-180270-MS. https://doi.org/10.2118/180270-MS.

Hoffman, B. T. 2018. Huff-n-puff Gas Injection Pilot Projects in the Eagle Ford. Presented at the SPE Canada Unconventional Resources Conference, Calgary, Alberta, Canada, 13-14 March. SPE-189816-MS. https://doi.org/10.2118/189816-MS.

Holm, L., and Josendal, V. 1974. Mechanisms of Oil Displacement By Carbon Dioxide. *J Pet Technol* **26**(12): 1,427 - 1,438. SPE-4736-PA. https://doi.org/10.2118/4736-PA.

Jamialahmadi, M., Emadi, M., and Müller-Steinhagen, H. 2006. Diffusion coefficients of methane in liquid hydrocarbons at high pressure and temperature. *Journal of Petroleum Science and Engineering*, *53*(1-2), 47-60. https://doi.org/10.1016/j.petrol.2006.01.011

Jin, L., Hawthorne, S., Sorensen, J. et al. 2017. Utilization of Produced Gas for Improved Oil Recovery and Reduced Emissions from the Bakken Formation. Presented at the SPE Health, Safety, Security, Environment & Social Responsibility Conference, New Orleans, Louisiana, 18-20 April. SPE-184414-MS. http://dx.doi.org/10.2118/184414-MS.

Kovscek, A. R., Tang, G., and Vega, B. 2008. Experimental Investigation of Oil Recovery From Siliceous Shale by CO2 Injection. Presented at the SPE Annual Technical Conference and Exhibition, Denver, Colorado, USA, 21-24 September. SPE-115679-MS. https://doi.org/10.2118/115679-MS.

Lansangan, R., and Smith, J. 1993. Viscosity, Density, and Composition Measurements of CO2/West Texas Oil Systems. *SPE Res Eng* **8**(03): 175 - 182. SPE-21017-PA. https://doi.org/10.2118/21017-PA.

Li, L. and Sheng, J. J. 2016. Experimental study of core size effect on CH4 huff-n-puff enhanced oil recovery in liquid-rich shale reservoirs. *Journal of Natural Gas Science and Engineering* 34: 1392-1402. https://doi.org/10.1016/j.jngse.2016.08.028.

Liu, G., Sorensen, J., Braunberger, J., et al. 2014. CO2-Based Enhanced Oil Recovery from Unconventional Reservoirs: A Case Study of the Bakken Formation. Presented at the SPE

Unconventional Resources Conference, The Woodlands, Texas, USA, 1-3 April. SPE-168979-MS. https://doi.org/10.2118/168979-MS.

Ma, Y.Z. 2015. Unconventional Resources from Exploration to Production. In *Unconventional Oil and Gas Resources Handbook: Evaluation and Development* Chap. 1, 3—52. Elsevier.

McGuire, P. L., Okuno, R., Gould, T. L. et al. 2017. Ethane-Based Enhanced Oil Recovery: An Innovative and Profitable Enhanced-Oil-Recovery Opportunity for a Low-Price Environment. *SPE Res Eval & Eng* **20** (01): 42 - 58. SPE-179565-PA. https://doi.org/10.2118/179565-PA.

Rao, D. and Lee, J. 2000. Miscibility Evaluation for Terra Nova Offshore Field. Presented at Canadian International Petroleum Conference, Calgary, Alberta, 4-8 June. PETSOC-2000-082. https://doi.org/10.2118/2000-082.

Rognmo, A., Fredriksen, S., and Ferno, A. 2017. Unlocking the Potential Without Fracking – CO2 Injection in Tight Shale Oil. Presented at the International Symposium of the Society of Core Analysts, Vienna, Austria, 27 August - 1 September.

Sinha, A. 2017. *Surface Area Study in Organic Rich Shales using Nitrogen Adsorption*. MS Thesis. University of Oklahoma, Norman, Oklahoma.

Song, C., and Yang, D. 2013. Performance Evaluation of CO2 Huff-n-puff Processes in Tight Oil Formations. Presented at the SPE Unconventional Resources Conference Canada, Calgary, Alberta, Canada, 5-7 November. SPE-167217-MS. https://doi.org/10.2118/167217-MS.

Sorensen, J. A., Pekot, L. J., Torres, J. A., et al. 2018. Field Test of CO_2 Injection in a Vertical Middle Bakken Well to Evaluate the Potential for Enhanced Oil Recovery and Co_2 Storage. Presented at the SPE/AAPG/SEG Unconventional Resources Technology Conference, Houston, Texas, USA, 23-25 July. URTEC-2902813-MS. https://doi.org/10.15530/URTEC-2018-2902813.

Srivastava, R. and Huang, S. 1997. Laboratory Investigation Of Weyburn CO2 Miscible Flooding. Presented at the Petroleum Conference of The South Saskatchewan Section, Regina, Canada, 19-22 October. https://doi.org/10.2118/97-154.

Stalkup, F. 1987. Displacement Behavior of the Condensing/Vaporizing Gas Drive Process. Presented at the SPE Annual Technical Conference and Exhibition, Dallas, Texas, 27-30 September. SPE-16715-MS. https://doi.org/10.2118/16715-MS.

Thomas, W., Helms, L., Driggers K. et al. 2016. EOG Resources (EOG) Earnings Call, May 06, 2016

Wang, L., Tian, Y., Yu, X. et al. 2017. Advances in improved/enhanced oil recovery technologies for tight and shale reservoirs. *Fuel* **210**:425-445. https://doi.org/10.1016/j.fuel.2017.08.095

Yin, M. 2015. *CO2 miscible flooding application and screening criteria.* MS Thesis. Missouri University of Science and Technology, Rolla, Missouri.

Yu, Y. 2016. *Experimental Study of Enhanced Liquid Oil Recovery from Shale Reservoirs by Gas Injection.* PhD dissertation, Texas Tech University, Lubbock, Texas.

Yu, Y., and Sheng, J. J. 2016. Experimental Investigation of Light Oil Recovery from Fractured Shale Reservoirs by Cyclic Water Injection. Presented at the SPE Western Regional Meeting, Anchorage, Alaska, USA, 23-26 May. SPE-180378-MS. https://doi.org/10.2118/180378-MS.

Zhang, F., Adel, I. A., Park, K. H., et al. 2018. Enhanced Oil Recovery in Unconventional Liquid Reservoir Using a Combination of CO2 Huff-n-puff and Surfactant-Assisted Spontaneous Imbibition. Presented at the SPE Annual Technical Conference and Exhibition, Dallas, Texas, USA, 24-26 September. SPE-191502-MS. https://doi.org/10.2118/191502-MS.

Appendix A: Details of experimental procedures

Preserved rock sample was crushed using metal pestle and mortar and sieved to obtain particle size of 7 to 8 mm. Around 22 gm of crushed sample was put in a glass vial and NMR T1 & T2 spectra were obtained. 12 MHz NMR apparatus was used. For T2 test, tau – 0.057 ms, T2 max = 100 ms. For T1/T2 test, tau - 0.057 ms, and T1=200 ms, and T2= 100 ms. After the NMR test is finished, the crushed sample was placed in the oven for two hours at 150°F. This step is necessary for not to include any loss due to evaporation due to the temperature effect in the 1^{st} cycle. After two hours, NMR test was again run to obtain base case NMR spectrum. Now the sample is ready to be placed in the high pressure cell for EOR study. The high pressure cell is rated to 10,000 psi and temperature of 212°F. High pressure cell with sample is place in an oven and the temperature is raised to 150°F. Sample is allowed to sit at this temperature prior to introduction of gas. The solvent gas cylinder valve and the valve on the top of the pressure cell is opened (see **Fig. 15**) to fill the ISCO 100DX syringe pump, the high-pressure cell and the high pressure tubing. After filling is complete, the gas cylinder valve is closed and the pump is started to builds up the desired injection pressure (P_{inj}). This represents the huff phase. Once the system reached the desired pressure $P_{inj,}$ the valve on the top of the pressure cell is closed to isolate the high pressure cell and allowed to sit for 1 hour (represent the soaking phase). After the desired soaking time, the outlet needle valve is opened to depressurize the cell to atmospheric pressure (puff cycle). This is achieved in one hour (production time). The crushed sample is taken out and placed in the desiccator for one hour and thirty minutes to allow the injected gas to escape from the samples. T_2 and T_1/T_2 NMR spectra are acquired. This constitutes one cycle. Using the same procedure as outlined above, data is obtained for successive cycles. Destructive tests such as MICP, BET, GC, and HAWK are performed after the last cycle of huff-n-puff tests.